博士論文

論文題目　An Essential Role of DNase II in DNA-sensing by TLR9

（TLR9 による DNA 認識における DNase II の役割）

氏　　名　　陳 美寶

An Essential Role of DNase II in DNA-sensing by TLR9

TLR9 による DNA 認識における DNase II の役割

Division of Innate Immunity, Department of Microbiology and Immunology, institute of Medical Science, The University of Tokyo
Supervisor: Prof. Kensuke Miyake

陳 美寶

Abstract

Deoxyribonuclease II (DNase II) digests DNA in endolysosomes. In the absence of DNase II, undigested DNA activates cytoplasmic DNA-sensing pathways. Little is known, however, about the role of DNase II in endolysosomal DNA sensing by TLR9. Here we show that DNase II is required for TLR9 responses. Two types of TLR9 ligands, CpG-A and CpG-B, were used. Only CpG-A responses were impaired in DNase II-deficient DCs. Enzymatically inactive DNase II mutants did not rescue CpG-A responses. DNase II cleaved CpG-A from 20mer to 11-12mer oligodeoxynucleotides. A synthetic 3' 11mer CpG-A fragment was able to activate DNase II-deficient DCs. Since CpG-A is reported to induce type I IFN production in LAMP-2^{+} lysosomes in conventional DCs, the localizations of endogenous DNase II and internalized CpG-A were examined. Results showed that CpG-A exhibited greater colocalization with LAMP-2^{+} lysosomes than CpG-B or the 3'11mer, CpG-A also increased DNase II trafficking to LAMP-2^{+} lysosomes. These results suggest that TLR9 responds to DNA fragments cleaved by DNase II.

Table of Contents

List of Abbreviations

APC	Antigen presenting cell
AGS	Aicardi-Goutières syndrome
BM	Bone marrow
cDC	Conventional dendritic cell
cDNA	Complementary DNA
DAI	DNA-dependent activator of IFN-regulatory factors
DDX41	DEAD box polypeptide 41
DEAD	Asp-Glu-Ala-Asp
DNA	Deoxyribonucleic acid
DOTAP	*N*-[1-(2,3-dioleoyloxy)]-*N*,*N*,*N*-trimethylammoniumpropan methylsulphate
EDTA	Ethylenediaminetetraacetic acid
EEA1	Early endosome autoantigen 1
ELISA	Enzyme-linked immunosorbent assay
ER	Endoplasmic reticulum
ESCRT	Endosomal sorting complex required for transport
FACS	Fluorescence-activated cell sorting
fH	FLAG-Histidine
Flt3L	Fms-like tyrosine kinase 3 ligand
GFP	Green fluorescent protein
GM-CSF	Granulocyte-macrophage colony-stimulating factor
HAT	Hypoxanthine-aminopterin-thymidine
HCl	Hydrochloric acid
HMGB	High-mobility group box
HT	Hypoxanthine-thymidine
IFA	Incomplete Freund’s Adjuvant
IFI16	Interferon-inducible protein 16
IFN	Interferon
IFNAR	IFN-α/β receptor
Ig-like	Immunoglobulin-like

IκB	Inhibitor of κB
IKK	IκB-kinase
IL	Interleukin
IL-1R	IL-1 receptor
IRAK	IL-1R-associated kinase
IRF	Interferon regulatory factor
kb	Kilobase
kDa	Kilodaltons
K63	Lysine 63
LAMP	Lysosome-associated membrane protein
LPS	Lipopolysaccharide
LRR	Leucine-rich repeat
mAb	Monoclonal antibody
MAPK	Mitogen-activated protein kinase
mDNA	Mitochondrial DNA
mRNA	Messenger RNA
MyD88	Myeloid differentiation primary-response protein 88
NF-κB	nuclear factor κ-light-chain-enhancer of activated B cells
NK	Natural killer
ODN	Oligonucleotide
PAMP	Pathogen-associated molecular pattern
PBS	Phosphate-buffered saline
PCR	Polymerase-chain reaction
pDC	Plasmacytoid dendritic cell
PDGF	Platelet derived growth factor
PRR	Pattern-recognition receptor
PVDF	Polyvinylidene difluoride
QPCR	Quantitative real-time PCR
RANTES	Regulated on activation, normal T cell expressed and secreted
RBC	Red blood cell
RIG-I	Retinoic acid-inducible gene I

RNA	Ribonucleic acid
SDS-PAGE	Sodium dodecyl sulfate -polyacrylamide gel electrophoresis
SLE	Systemic lupus erythematosus
SNP	Single nucleotide polymorphism
STING	Stimulator of interferon genes
TAK1	transforming growth factor-β activated kinase 1
Th1	T helper type 1
TIR	Toll–IL-1R
TLR	Toll-like receptor
TM	Transmembrane
TNF	Tumor necrosis factor
TRAF	TNF receptor associated factor
Trex1	Three prime repair exonuclease 1
TRIF	TIR-domain-containing adapter-inducing interferon-β
Unc93B1	Unc-93 homolog B1
WGA	Wheat germ agglutinin

Acknowledgements

I would like to express my deepest gratitude to my supervisor, Prof. Kensuke Miyake, for his support and excellent supervision. His valuable advice and guidance have made this thesis possible.

I also want to thank Dr. Shin-Ichiroh Saitoh, who is a very generous person and devoted to his research work. He has provided me with a lot of technical support and advices. Dr. Ryutaro Fukui is another person that I must thank. I have learnt many experimental techniques from him. He has given me many useful comments for how to plan and organize my own experiments. Special thanks to Dr. Natsuko Tanimura, who also gave me many useful suggestions for my project. Ms. Haruyo Moriya, who is the secretary in our laboratory, has helped me a lot in accommodating the life in Tokyo, which is not easily adaptable for a foreigner.

Further, I would like to thank other labmates in our laboratory for their support and encouragement. I am really glad to know them.

I also would like to thank my dear great friends, some of them are, May, Karen, Irene, Mimi and Peggy for their unlimited support and love. Many thanks to my family members, without your love and considerations, I would not be strong enough to overcome the challenges and frustrations during the stay outside my home-Hong Kong. This work is also devoted to my beloved father. I love you all.

Last but not least, I would also like to acknowledge the Todai Fellowship from the University of Tokyo for financing my life in Japan.

1. Introduction

1.1 Innate and adaptive immunity

The mammalian immune system is comprised of two interrelated arms of responses, namely, the innate and adaptive immune systems. The innate immune system is the first-line of defense against microbes [1]. This system allows the host immediate action towards pathogens. This is achieved by a set of germ-line encoded receptors known as the “pattern recognition receptors” (PRRs), which detect microbial components conserved among pathogens (collectively regarded as pathogen-associated molecular patterns, PAMPs) [2]. Antigen-presenting cells (APCs) such as macrophages and dendritic cells are the main inducers and effectors in this system. Upon stimulation through the PRRs, they are capable of mediating inflammatory responses at the site of infection. In addition, these APCs undergo maturation and antigen processing, presenting the captured antigens to cells in the adaptive immune system [3]. Upon epitope recognition with their surface receptors, specific clones of B and T lymphocytes swiftly proliferate and differentiate into effector cells. Even after antigen clearance, a small number of these lymphocytes persist as memory cells, which provide long-lasting protective immunity against subsequent encounter of the same antigen [4, 5]. In addition to the PRRs from APCs, PRRs from adaptive immune cells can also directly trigger the cells to mount an immune response [6, 7]. In general, productive immune responses require the interactions between these two arms with delicate controls.

1.2 Innate pathogen sensors

To detect the numerous pathogens in our surrounding environment, the innate immune system has to equip with a broad array of sensors that detect different components of the pathogens. The initially identified innate receptor is the Toll-like receptor (TLR) family, which consists of specialized family members responsible for sensing lipids, proteins and nucleic acids from microbes. Subsequently, cytosolic receptors for nucleic acids were also identified, which include the retinoic acid-inducible gene I (RIG-I) like receptor family for sensing cytosolic RNA, and various cytosolic DNA sensors. In the latter category, a number of candidates have been identified, such as the DNA-dependent activator of interferon (IFN) (DAI) regulatory factors, Asp-Glu-Ala-Asp (DEAD) box polypeptide 41 (DDX41) and IFN-inducible protein 16 (IFI16) [8]. Recently, a seminal progress on intracellular DNA sensing has been the identification of the dinucleotide cyclic-GMP-AMP (cGAMP) synthase (cGAS) [9], which generates cGAMP, the ligand that can directly stimulate the common adaptor protein called stimulator of interferon gene (STING) [10]. STING resides on the endoplasmic reticulum (ER) membrane and upon detection of upstream messenger, activates the transcription factor nuclear factor κ-light-chain-enhancer of activated B cells (NF-κB) and IFN regulatory factor 3 (IRF3), resulting in production of type I IFN and proinflammatory cytokines [11].

1.3 The DNA-sensing TLR9

The Toll receptor was initially discovered in *Drosophila melanogaster* for controlling embryonic patterning and immune responses in the organism [12]. However, in mammals, TLRs are specialized in immune defense [13]. TLRs, like the Drosophila Toll, are evolutionarily conserved type I transmembrane (TM) receptors that bear an

ectodomain made up of leucine-rich repeats (LRRs) domain for PAMPs detection (Figure 1). Each TLR consists of 19-25 tandem LRR motif, and each LRR contains 24-29 amino acids. Following the LRRs are the cysteine-rich motif, the TM region and the intracellular Toll-interleukin-1 receptor (TIR) domains. Due to the conserved nature of the TIR domain between interleukin-1 receptor (IL-1R) and TLRs, they share similar downstream signaling pathways [14, 15]. There are currently 13 known TLRs in the mammalian genome (TLR1-13). Their respective ligands and subcellular localizations are briefly depicted in Figure 2.

There is only one DNA sensor within the TLR family, TLR9, which is found in the endosomes in the steady state (Figure 2a). It was initially discovered as a receptor for bacteria-derived DNA containing unmethylated CpG motifs [16]. Later, the target of TLR9 has been extended to viral CpG-rich DNA as well [17]. Since CpG DNA is potent in stimulating TLR9 in immune cells to produce T helper type 1 (Th1) cytokines, such as IL-12 [18-20], it is commonly used as an adjuvant in vaccines against infections or tumors [21, 22].

1.4 TLR9-stimulating ligands

Before the discovery of TLR9, synthetic CpG oligodeoxynucleotides (ODNs) have been developed as immunostimulants for clinical purposes [23, 24]. Later, the receptor for these ODNs was found to be TLR9 [16]. Currently, there are three major types of CpG ODNs: CpG-A, CpG-B and CpG-C. CpG-C can be considered as a combination of the properties from CpG-A and CpG-B. These three types of CpG DNA have in common the stimulatory CpG motif made up of the sequence formula "purine-purine-CG-pyrimidine-pyrimidine" [25]. Experimental analyses revealed that the best sequence for stimulating various species contains GTCGTT. The stimulatory

effect is enhanced when the optimal sequence is preceded by a TC dinucleotide at the 5’ end and followed by pyrimidine-rich sequences at the 3’ end [25]. The three classes of ODNs differ in terms of nucleotide sequences and backbone modifications [26-28]. CpG-A has a central palindromic sequence and poly-G at both the 5’ and 3’ ends. These poly-G sequences are phosphorothioated (nuclease resistant) in each of the CpG-A subtypes (Table 1). For CpG-B, all the bases are phosphorothioated and there is no central palindrome as that found in CpG-A. On the other hand, nucleotides in CpG-C are all phosphorothioate (PS)-modified with palindromic sequence near the 3’ end (Table 1).

The effects of CpG-A and CpG-B also differ as they tend to stimulate different cell types and induce different inflammatory responses. CpG-A is potent in inducing the type I interferon (IFN), while CpG-B strongly activates the NF-κB pathway [27, 29, 30]. Oligodeoxynucleotides with phosphodiester (PO) backbones are believed to be more potent in stimulating plasmacytoid dendritic cells (pDCs) and natural killer (NK) cells [27]. Plasmacytoid dendritic cells are known to respond to CpG-A vigorously with the production of IFN-α, which in turns activate NK cells [31]. The nuclease-resistant PS-modified ends render a longer half-life of CpG-A in stimulating the cells. To unravel the potency of CpG-A in inducing massive production of IFN in pDCs, Kerkmann and others have demonstrated that both the central palindrome and the poly-G motifs cooperatively form a stable tertiary structure that resembles a virus particle [32]. Such nucleic acid-based nanoparticle strongly induces IFN-α production, and that CpG-B-coated polystyrene nanoparticle also gains the potency of IFN-α induction as that of CpG-A [32]. Thus, forming aggregated structure appears to be important in IFN induction.

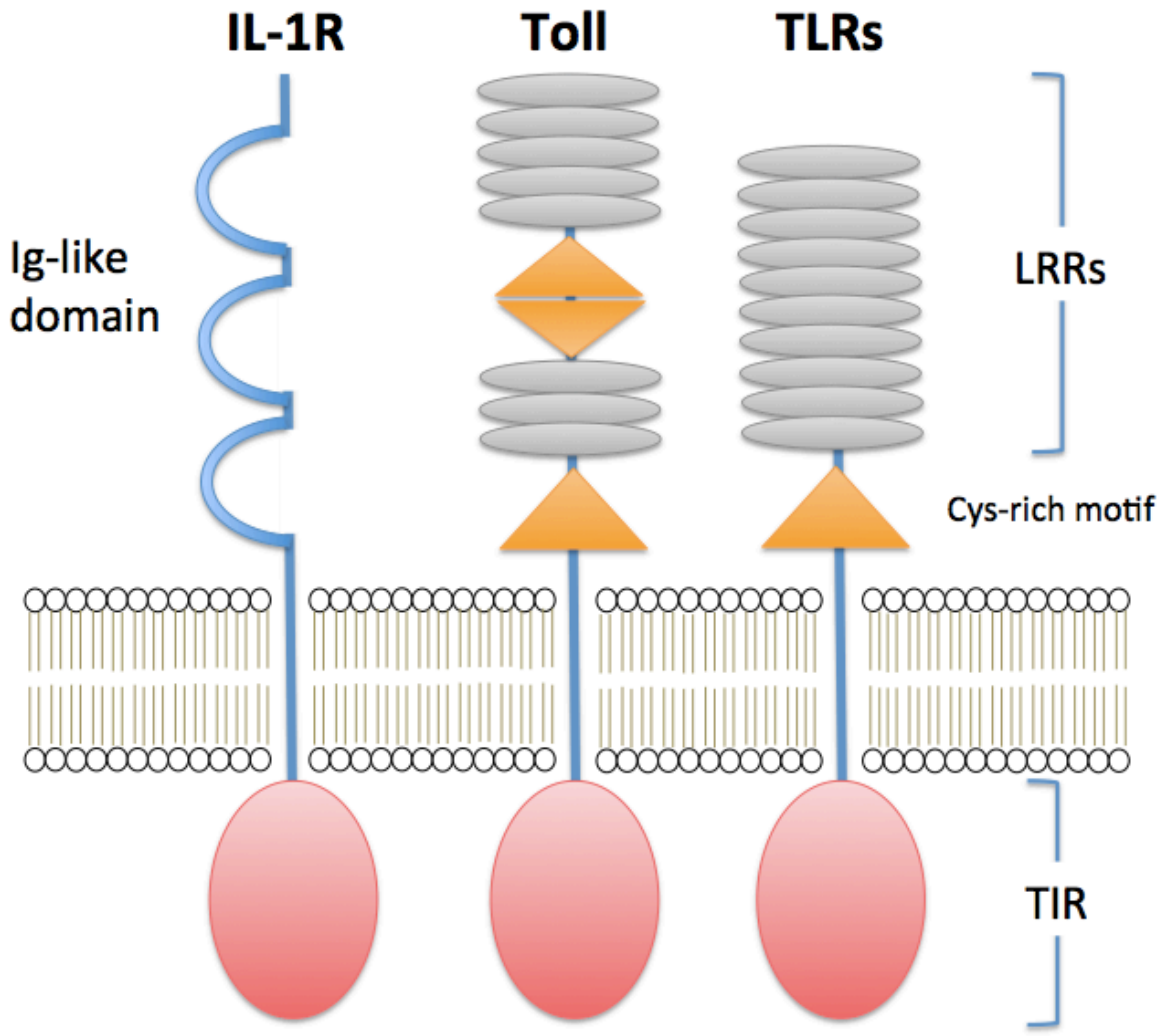

Figure 1. The structural differences and similarities between the three types of inter-related receptors. The ectodomain of IL-1R is composed of three tandem Ig-like motifs, which is tremendously different from that of the Drosophila Toll and mammalian TLRs, indicating the difference in the nature of ligand bindings. IL-1R binds to the proinflammatory cytokine IL-1β, whereas the Drosophila Toll binds to a cleaved internal protein called Spatzle in response to PAMPs [33, 34]. The mammalian TLRs are close relatives of Toll that are able to bind to PAMPs directly. The three types of receptors share a conserved TIR domain, thus recruiting similar repertoires of signaling adaptors and firing similar responses.

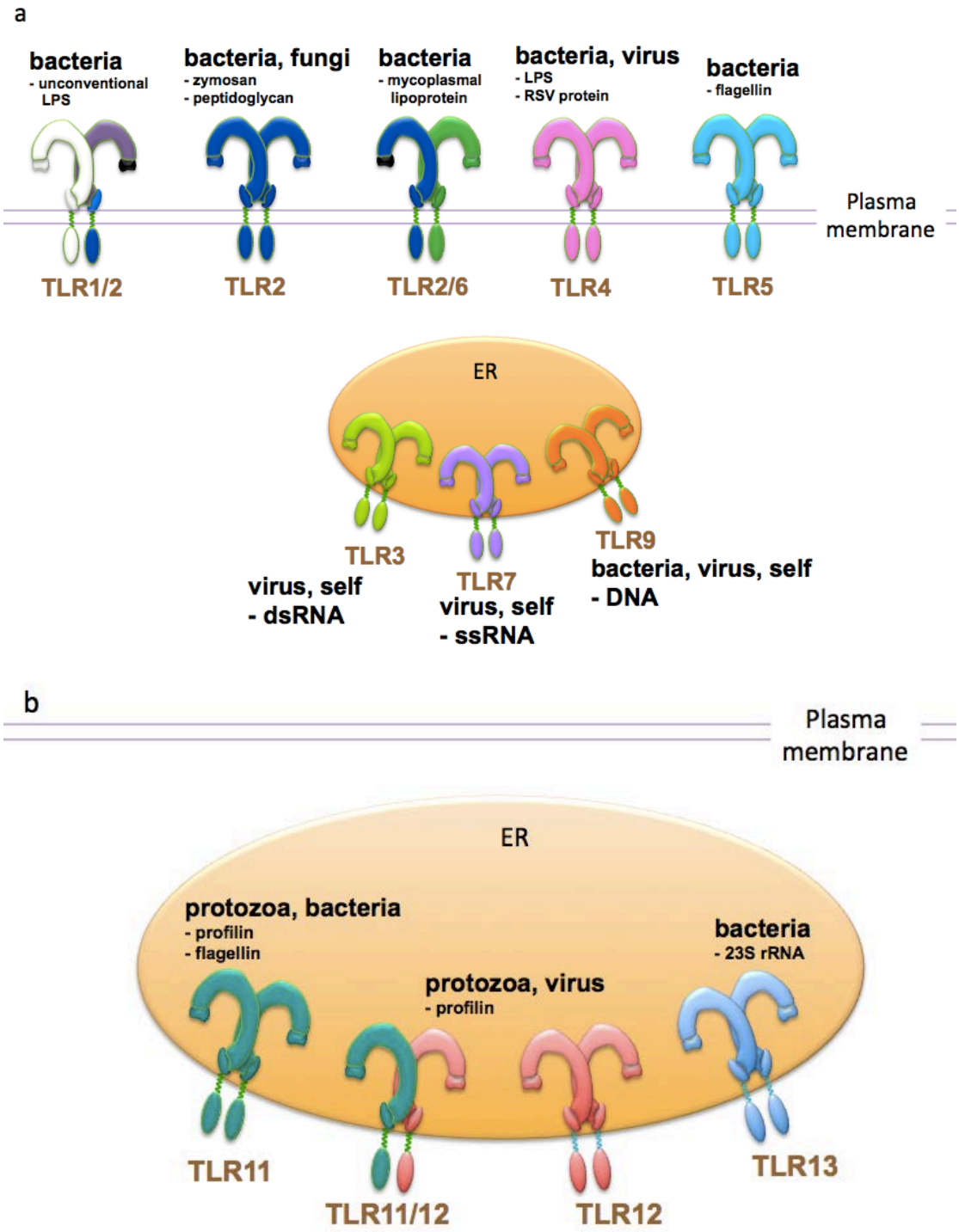

Figure 2. Subcellular localizations and representative ligands of the murine TLR family. (a) The surface TLRs (TLR1-6) have been found to detect bacterial cell wall components. TLR1/2 and TLR2/6 forms heterodimers that recognize bacterial lipids, while other TLRs form homodimers [35]. The intracellular TLRs (TLR3, 7, 9) are devoted to the recognition nucleic acid from viruses or bacteria. (b) TLR11-13 are also localized in endosomal compartment. TLR11 and TLR12 can form homodimer or heterodimer with each other. TLR13 has only been found to form homodimer with itself.

ODNs	5'-3' sequence	Species specificities	References
1585	ggGGTCAACGTTGAgggggg	Mouse	[29]
2216	ggGGGACGATCGTCgggggg	Human/mouse	[36]
2336	gggGACGACGTCGTGgggggg	Human	[37]
684	tcgacgttcgtcgttcgtcgttc	Human/mouse	[38]
1668	tccatgacgttcctgatgct	Mouse	[25]
2006	tcgtcgttttgtcgttttgtcgtt	Human	[36]
2395	tcgtcgttttcggcgcgcgccg	Human/mouse	[39]
M362	tcgtcgtcgttcgaacgacgttgat	Human/mouse	[22]

Table 1. Examples of different subtypes of CpG-A (1585, 2216 and 2336; shaded in pink), CpG-B (684, 1668 and 2006; shaded in green) and CpG-C (2395 and M362; shaded in blue). The species specificities are mainly determined empirically. The palindromic sequences are underlined, with phosphodiester bonds represented by capital letters and lower cases the phosphorothioated bases.

1.5 TLR9 activation and downstream signaling cascades

TLR9 has to be transported to the site where DNA is internalized. Unc-93 homolog B1 (Unc93B1) is an ER-resident transmembrane glycoprotein that carries TLR9 to the ligand-containing endolysosomal compartments [40]. After the ligand is delivered to endolysosomal compartments where TLR9 is present, TLR9 has to be proteolytically cleaved by cathepsins to its active form for signalling [41-44].

The TLR family employs two different types of signaling pathways, namely the myeloid differentiation primary-response 88 (MyD88)-dependent and the TIR-domain-containing adapter-inducing interferon-β (TRIF)-dependent pathways [14]. However, TLR9, similar to the endosomal RNA sensor TLR7, only relies on the MyD88-dependent pathway to mediate downstream signals [45] (Figure 3).

Engagement of MyD88 to the TIR domain of TLRs recruits the IL-1R-associated kinase 4 (IRAK4), IRAK1, and IRAK2 in a sequential manner. This complex in turn interacts with the tumor necrosis factor (TNF) receptor associated factor 6 (TRAF6). Recent reports suggest that TRAF6 transmits downstream signals with two different modes of actions: oligomerization with IRAK1 or production of K63-linked polyubiquitin chain [46, 47]. Either mode of action by TRAF6 leads to the activation of the downstream kinase, the transforming growth factor-β activated kinase 1 (TAK1). TAK1 then activates both the mitogen-activated protein kinases (MAPKs) and the inhibitor of kappa B (IκB) kinase (IKK) complex. The latter leads to the nuclear translocation of NF-κB. Both the MAPKs and IKK activations are essential for the induction of inflammatory cytokines by TLR9 [48, 49]. The major inflammatory cytokines produced are IL-6, IL-12p40 and TNF-α.

The MyD88-dependent pathway can also result in the production of type I IFN by recruiting the IRF family of transcription factors. Depending on the type of

immune cells, different IRFs are used [45, 50, 51]. In pDCs, TLR9 can induce exceptionally large amount of IFN-α through IRF7 and the TRAF6 complex. Some of the signaling molecules such as IRAKs and TRAF6 are also used in NF-κB activation [52]. However, in case of macrophages and conventional dendritic cells (cDCs), signals fired from TLR9 also induce type I IFN (IFN-β for cDCs), but only IRF1 is used [51].

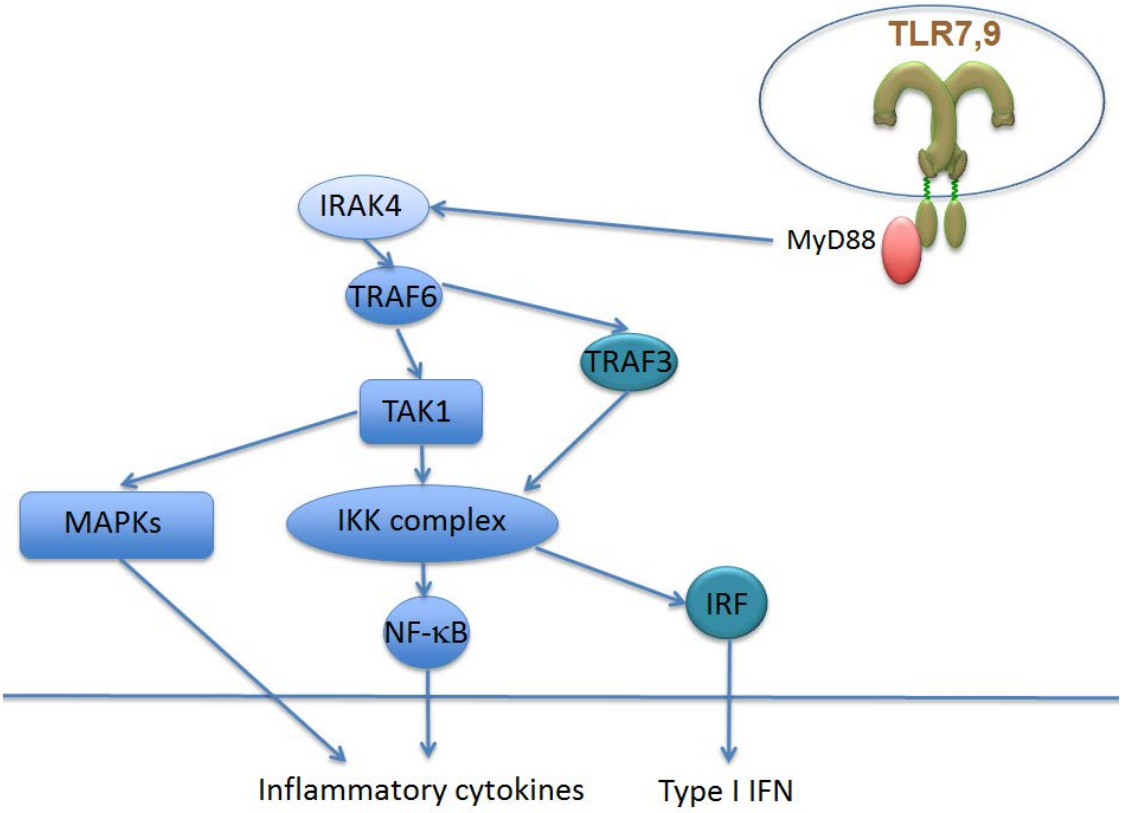

Figure 3. Simplified signaling pathways of TLR9. TLR7 and TLR9 are the endosomal TLRs that both employ MyD88 as a relay to recruit further signaling molecules. The NF-κB and MAPKs are required for inflammatory cytokine productions whereas IRFs are induced for type I IFN production. The specific IRF involved is cell-type specific.

1.6 Roles of DNase in immune diseases

Due to the constant surveillance by a multitude of DNA sensors in our body, DNases have to function properly to ensure normal DNA degradations. Previous reports have shown that mutations or polymorphisms in DNase I predispose to systemic lupus erythematosus (SLE) in humans [53, 54] and mice [55]. In the *Dnase1*$^{-/-}$ mice, production of anti-nuclear antibodies and the deposition of immune complexes in the kidney have been reported [55].

The acid DNase, DNase II, is found to be a key suppressor of STING functions in normal physiological conditions [56]. Kawane and coworkers have demonstrated that DNase II is required for digesting engulfed apoptotic DNA in liver phagocytes [57]. In the absence of DNase II, DNA is accumulated in lysosomes and stimulates STING to release a large amount of IFN-β, which causes premature death of the embryo [56, 58]. For double-ablation of DNase II and the type I IFN receptor (*Dnase2a*$^{-/-}$ *Ifnar1*$^{-/-}$), although the mice survive and only slightly anaemic, they develop chronic polyarthritis with age [59]. Other study also relates DNase II polymorphism to complications developed in SLE patients [60]. Since SLE is caused by the production of autoantibodies against apoptotic DNA [61], and DNase II-deficient mouse embryos accumulate undigested DNA in phagocytes found in various tissues [57, 62], it is plausible that DNase II may play some roles in SLE.

DNase III (also known as the 3' repair exonuclease 1, Trex1) is another DNase that is involved in type I IFN-related autoimmune disease in human, called the Aicardi-Goutières syndrome (AGS) [63]. Mutations of DNase III in human autoimmune diseases have also been documented [64].

1.7 TLR9 and DNase II

Since TLR9 responds to DNA in lysosomal compartments [65], it is possible that the lysosomal DNase II contributes to TLR9 responses, either to enhance or attenuate, by modifying the DNA ligands. Oka *et al*. have noticed that DNase II is crucial in the clearance of mitochondrial DNA (mDNA) leaked during haemodynamic stress in cardiomyocytes. Failure to timely remove the mDNA activates TLR9 and induces cardiac inflammation. This can ultimately lead to myocarditis and dilated cardiomyopathy characteristics of heart failure [66].

As the role of DNase II in cytosolic DNA sensors regulation has been revealed, it is intriguing to investigate the function of DNase II in the endosomal counterpart of DNA sensor, the TLR9, in immune cells. The fact that TLR9 does not cause lethal inflammation in *Dnase2a*$^{-/-}$ mice [67] suggests that regulation of TLR9 responses may involve more complicated manipulation of the ligand. Since DNase II digests DNA in lysosomes [68], and that TLR9 is also found in lysosome after stimulation with CpG DNA [69, 70], I examined the mechanism underlying DNA sensing by TLR9 in relation to DNase II. The present study shows that DNase II is indeed required for TLR9 responses upon stimulation with its conventional IFN-inducing ligand, CpG-A.

2. Materials and Methods

2.1 Mice

The wildtype (WT) mice were purchased from Japan SLC. The *Tlr9*$^{-/-}$ mice were a gift from Prof. Shizuo Akira's lab (Osaka University, Osaka, Japan). The *Ifnar1*$^{-/-}$ mice were purchased from B&K Universal, while the *Dnase2a*$^{+/-}$ mice were purchased from RIKEN BioResource Center. The *Dnase2a*$^{-/-}$ *Ifnar1*$^{-/-}$ mice were generated by mating the *Dnase2a*$^{+/-}$ and *Ifnar1*$^{-/-}$ mice. The DNase II conditional KO mice (*Dnase2a*$^{flox/+}$) was also purchased from RIKEN BioResource Center [59]. The *Dnase2a*$^{flox/flox}$ *Tie2 Cre* mice were generated by mating *Dnase2a*$^{flox/+}$ and *Tie2-Cre* transgenic mice (Jackson Laboratory). All the mice were either purebred or inbred to a C57BL/6 background. The animals were kept in a specific pathogen-free environment within the animal facility in the Institute of Medical Science, the University of Tokyo. All animal experiments were approved by the Animal Care and Use Committee, strictly performed in accordance to the institutional ethical guidelines issued by the University of Tokyo.

2.2 Cell lines

The pro-B cell line Ba/F3 derived from the C3H mice was used in this study for murine DNase II protein production. It is cultured in complete RPMI medium 1640 (10% fetal calf serum, FCS; 1X penicillin-streptomycin-glutamine; 50μM 2-mercatoethanol, 2-ME) supplemented with IL-3, and maintained in 37°C CO_2 incubator. Plain RPMI medium 1640, FCS and penicillin-streptomycin-glutamine were purchased from Gibo. 2-ME was from Nacalai Tesque Inc.

2.3 TLR9 ligands

CpG-A (2216, sequence 5'-ggGGGACGATCGTCgggggg-3'), CpG-B (1668, sequence 5′-tccatgacgttcctgatgct-3′) and other ODNs were synthesized by Hokkaido System Science. Nucleotides in upper case represent phosphodiester linkage, whereas those in lower cases were in phosphorothioate bonds, which are nuclease-resistant. In some of the treatments, CpG ODN was pre-incubated with lipofectamine 2000 Reagent (Invitrogen) at room temperature for 20 minutes, following the manufacturer's instructions before added to cells.

2.4 Murine DNase II protein

Ba/F3 expressing the murine *Dnase2a* with a FLAG-His (fH) tag at the C-terminus was made. Culture supernatant from these cells was collected and purified with FLAG peptide (DDDDK peptide) (MBL International). To quantify the purified proteins, a small amount of each of the proteins was analyzed by Sodium dodecyl sulfate - polyacrylamide gel electrophoresis (SDS-PAGE) and silver-stained (silver-staining reagents purchased from Invitrogen). The band intensities were then measured using Photoshop (Adobe).

2.5 DNase II activity assay

The DNA digestion activities of the purchased porcine DNase II, or the purified WT and mutant murine DNase II were determined by adding 10-50ng of the proteins into the activity reaction buffer (10mM Tris/HCl pH5.3, 5mM EDTA pH8.0) with 500ng of 6kb DNA plasmid and incubated at 37°C for 1 hour. The results were visualized by agarose gel electrophoresis with 1% agarose gel pre-stained with ethidium bromide.

2.6 Vector constructions

The WT *dnase2a* coding sequences was obtained by Polymerase-chain reaction (PCR) using primary dendritic cells complementary DNA (cDNA) as template. It was then subcloned into the pMX, pMXpuro or pMXneo vector with FLAG-His (fH) tag at the 3' end. The DNase II mutants H115A, H132A and H297A were generated by the site-directed mutagenesis with the PrimeSTAR Max PCR kit (TaKaRa), using the WT DNase II inserted into pMD20-T vector (empty vector from TaKaRa) as template. For the mutagenesis, the primer sets used for the various mutants is listed in Table 2.

Site of mutation	Primers set used	Amino acid change
115	Fw: CATGGGGCAACGAAGGGTGTCCTGCTC Rv: CTTCGTTGCCCCATGGCCGGTAGAGTC	Histidine→Alanine
132	Fw: CTGGTCGCCAGTGTGCCTCGCTTCCCA Rv: CACACTGGCGACCAGCCAGAAGCCCCC	Histidine→Alanine
297	Fw: GAGGACGCATCCAAATGGTGTGTGGCC Rv: TTTGGATGCGTCCTCTGTGGCACTGAA	Histidine→Alanine

Table 2. Primers used to introduce the amine acid mutations in the murine DNase II. The underlined primer sequences represent the amino acid being changed.

2.7 Retroviral transduction

The respective vector was transfected into the Plat-E retroviral packaging cell line following the instructions from FuGene 6 (Roche). Two days after transfection, the viral supernatant in complete DMEM was collected. For transduction, the supernatant was added to the cells with the liposome DOTAP (Roche). The culture plate was then centrifuged at 2,000 rpm for 60 minutes.

2.8 Reverse transcription and quantitative real-time PCR

Cellular RNA was purified using the RNeasy Mini Kit (Qiagen) and then reverse transcribed to cDNA with ReverTra Ace qPCR RT Kit (Toyobo). The resulting cDNA was relatively quantitated with the TaqMan probes for β-actin or DNase II (all obtained from Applied Biosystems) using the machine StepOnePlus Real Time PCR System (Applied Biosystems).

2.9 ELISA

The production of IFN-α, IL-12p40 and RANTES were all measured using the ELISA kits from R&D Systems.

2.10 Co-immunoprecipitation and Western blotting

Cells were collected and washed twice with phosphate-buffered saline (PBS). The cell pellets were lyzed with lubrol lysis buffer (1% lubrol, 150 mM NaCl, 50 mM Tris/HCl pH 7.4, 5 mM EDTA pH 8 and complete proteinase inhibitor from Roche). Lysates were incubated on ice for 30 minutes with occasional vortexing. They were then centrifuged at 150,000 rpm with a bench-top centrifuge (Kubota) for 15 minutes pre-cooled at 4°C. In the meantime, sepharose-conjugated antibodies were washed

briefly in PBS and then lysis buffer before added to cell lysates. The mixtures were allowed to rotate in cold room for 1.5-2 hours before washing. After immunoprecipitation, the mixtures were washed three times with 0.1% lubrol washing buffer (0.1% lubrol, 150 mM NaCl, 50 mM Tris/HCl pH7.4, 5 mM EDTA pH8), and boiled with 2x sample buffer (0.1M Tris/HCl pH6.8, 20% glycerol, 10% SDS, 6% 2-ME, 0.05% bromophenol blue) at 98°C for 8 minutes. The NHS-activated sepharose 4 fast flow (GE Healthcare)-conjugated antibodies that were used for immunoprecipitation included: mouse anti-TLR9 N-terminal (B33A4) or C-terminal mAbs (C34A1) (both generated in our laboratory) [71], mouse anti-DNase II mAbs (#5-38 and #17) and mouse anti-FLAG mAb (M2, purchased from Sigma-Aldrich).

For Western blotting, the boiled lysates were subjected to the standard SDS-PAGE procedures and the proteins on the gel were transferred onto a polyvinylidene difluoride (PVDF) membrane, blocked with 2.5% skim milk in TBS-T (50mM Tris, 150mM NaCl and 0.05% Tween-20, adjusted to pH7.4) and immunoblotted. The antibodies used include: rabbit anti-TLR9 TIR domain pAb made by Matsumoto F. in our laboratory; rabbit anti-GFP pAb (MBL International) and mouse anti-FLAG tag M2 mAb (Sigma-Aldrich). The signal was developed using the ECL Select Western blotting Detection Reagent and image captured with ImageQuant LAS500 (both GE Healthcare).

2.11 Flow cytometry analysis

Splenocytes were obtained by mechanical disruption of the whole spleen. The suspended cells were then passed through a mesh and red blood cells (RBCs) removed by lyzing with the RBC lysis buffer (0.144M NH_4Cl, 0.017M Tris, pH7.2) (room temperature for 3 minutes). For surface staining of BM-pDCs and BM-cDCs,

cells were pre-incubated with anti-CD16/32 antibodies in fluorescence-activated cell sorting (FACS) buffer (2.5% FCS, 0.02% $NaHCO_3$ and 0.1% NaN_3 in PBS) to block the endogenous Fc receptors to avoid non-specific antibody binding. Cells were stained with the following antibodies purchased from eBioscience: CD11b-FITC (M1/70), CD11c-PE (N418) and B220-APC (RA3-6B2). For checking the monoclonal antibody immunoglobin (Ig) subclasses and the type of light chain, the following antibodies were used: anti-IgG1 (A85-1, BD Pharmingen), anti-IgG2a (m2a-15F8, eBioscience), anti-IgG2b (RMG26-1, Biolegend), anti-IgM (II/41, eBioscience), anti-kappa (RMK-12, Biolegend) and anti-lambda (RML-42, Biolegend). All staining procedures were performed at 4°C for 15 minutes. The stained samples were analyzed using the BD Biosciences FACSCalibur cytometer and FlowJo software.

2.12 Bone marrow cell preparation

Murine bone marrow-cDCs (BM-cDCs) were cultured in complete RPMI medium 1640 supplemented with 10ng/ml recombinant murine granulocyte-macrophage colony-stimulating factor (GM-CSF) (Peprotech). BM-pDCs were cultured in complete RPMI medium 1640 supplemented with Fms-like tyrosine kinase 3 ligand (Flt3L) (Peprotech) at 100ng/ml. Both BM-cDCs and BMDMs were used for experiments on the 7^{th} day of culture. For BM-pDCs, on Day 7, they were double-stained with CD11c-PE (N418) and B220-APC (RA3-6B2) in culture medium before sorting with FACSAria cell sorter from BD Biosciences. The purity of pDCs was over 93% after sorting.

2.13 Bone marrow stem-cell transduction

On Day 1, fluorouracil (5-FU) (Kyowa) was injected intraperitoneally (at 5mg/head) into the mice to kill the actively dividing mature cells in the bone marrow. On Day 4, plasmids of interest were transfected into Plat-E for retrovirus packaging. Mice were sacrificed on the next day and the BM cells were obtained and maintained in stem cell medium (15% FCS, 10% sodium pyruvate, 1X penicillin-streptomycin-glutamine, 0.1% 2-ME, 0.01% IL-3, 0.01% IL-6 and 0.1% Stem Cell Factor in plain DMEM). On Day 7, viral supernatant was collected and transduced into the stem cell with 50μl of the reagent premix (0.1% IL-3, 0.1% IL-6 and 1% Stem Cell Factor in 50μl of sodium pyruvate) added per well. The transduction procedure was repeated once more on the next day. GM-CSF was then added to induce differentiation in cDCs. Cells were used for treatments on Day 21.

2.14 Generation of the anti-mouse DNase II mAbs

The mAbs were established by immunizing a *Dnase2a*$^{-/-}$*Ifnar1*$^{-/-}$ mouse with the purified WT mDNase II-fH protein mixed with CFA (*v*:*v*=1:1) intraperitoneally and also injected to the animal's footpad. The same protein mixture with Incomplete Freund's Adjuvant (IFA) was used as the boost two weeks later. The mDNase II-fH protein mixed with PBS was injected as further boost intraperitoneally and intravenously once a week for three more weeks. The immunized mouse was sacrificed one week after the final boost, and spleen cells were fused with the murine myeloma cell line SP2/O-Ag in a ratio of 5:1; while cells from lymph nodes were fused with SP2/O-Ag at 7:1. Polyethylene Glycol 1500 (Roche) was first added to the dispersed cell mixture pellet gently and slowly, after that, 12 ml of pre-warmed plain RPMI medium 1640 was also added carefully over a period of 5 minutes. After

removing the medium by centrifugation, the fused cells were seeded into 96-well plate. The hypoxanthine-aminopterin-thymidine (HAT) medium was added for selection 24 hours later.

Ab screening started when the cell colonies were visible by bare eyes. The culture supernatant from the hybridomas was tested for the presence of the anti-mDNase II antibody. FACS screening was done by using the Ba/F3 cells with forced expression of WT mDNase II on the cell surface by subcloning into the pDisplay vector (Life Technologies). Protein that is expressed from the pDisplay vector has a murine Ig-κ-chain leader peptide at the N-terminus, which directs the protein to the secretory pathway. The C-terminus of the protein is fused to the platelet derived growth factor receptor (PDGFR) transmembrane domain, so that it is anchored to the plasma membrane. Positive clones only for WT mDNase II were selected and expanded into 24-well plate in hypoxanthine-thymidine (HT) medium. Cells were stocked at this stage. Thymocytes from young BALB/c mice were obtained and seeded as feeder cells for hybridoma limiting dilution. The single-cell colonies were screened again for confirmation. Two mAbs (#5-38 and #17) were isolated.

2.15 Purification of mAbs

The monoclonal hybridomas were injected separately into the nude mice (Crlj:CD1-Foxn1^{nu}, purchased from Charles River Inc. Japan). One week after injection, ascites fluids were collected. To purify the mAbs, the ascites fluid from each of the mAbs was first centrifuged at 3,000 rpm for 30 minutes at 4°C. Two volumes of sodium acetate buffer (60mM sodium acetate, 29.5% acetic acid, adjusted to pH4.0 with HCl) were added and mixed by inverting. To precipitate impurities, amount of octanoic acid (Wako) equivalent to 0.04 volume of the ascites fluid was gently dripped into the

above mixture and shook on a seesaw shaker (at a speed of about 30 rpm) at room temperature for 30 minutes. After incubation, the mixture was centrifuged again for 3,000 rpm for 30 minutes at 4°C. If the supernatant was not clear after centrifugation, additional octanoic acid has to be added in a unit of 0.01 volume of the ascites fluid, and repeat the incubation step again. This procedure was repeated until a clear supernatant was attained. After centrifugation, the supernatant was filtered through a 0.45μm (non-sterile) and dialyzed against 1xPBS (about 2 litres) in cold room for overnight. On the next day, a second dialysis was performed by changing a newly prepared 1xPBS. The mAbs were dialyzed for the third time by changing another new volume of 1xPBS in the evening. On the following day, the dialysates were filtered through a 0.2μm filter (sterile). To determine the concentrations, optical density (OD) at 280nm (OD280) of 10x diluted dialysate was measured (OD280 of the value 0.146 was calculated as 1mg/ml of mAb). Presence of the purified mAb was verified by running an SDS-PAGE and the gel stained with coomassie blue. The purified mAbs were label with biotin-XX, SE (Molecular Probes) and conjugated to the NHS-activated sepharose 4 fast flow (GE Healthcare) for other applications.

2.16 Fluorescent CpG-A or CpG-B uptake assay

Fluorescein isothiocyanate (FITC)-conjugated CpG-A or CpG-B (Hokkaido System Science) was added to the cells seeded on a 24-well plate. The mixture was immediately chilled at 4°C for 30 minutes. After that, the culture was returned to the 37°C CO_2 incubator and incubated for the time indicated. Before FACS analysis, the cells were collected and washed twice in PBS. The fluorescent CpG clinging to the cell surface was quenched by trypan blue (Gibco) at 62μg/ml (diluted with PBS) for about 5 minutes before flow cytometry analysis [72].

2.17 CpG-ODN digestion assay

CpG-A or CpG-B was incubated with purified murine DNase II protein in sodium acetate reaction buffer (50mM sodium acetate pH4.66 plus 5mM EDTA pH8.0) for 24 hours at 37°C. Cleaved DNA was analysed by running in 20% Tris/Borate/EDTA (TBE) gel and stained with GelRed nucleic acid stain (Biotum) following the maker's instructions.

2.18 Confocal microscopy

Cells were seeded onto a glass-bottom plate (Greiner bio-one) overnight and fixed on the next day with 4% paraformaldehyde for 20 minutes. After permeabilization with 0.2% saponin in PBS for 8 minutes at room temperature, cells were stained with the following antibodies in combinations or separately: calnexin (abcam), EEA1 (Cell signaling), LAMP1-eFluor660 (eBio1D4B, eBioscience), LAMP2-eFluor660 (eBioABL-93, eBioscience), wheat germ agglutinin-Alexa Fluor 594 (Life Technology), mDNase II (#5-38, #17). Anti-DNase II #5-38 and #17 were used at 10μg/ml. All staining procedures were performed at room temperature. The fluorescent CpG ODNs were purchased from Hokkaido System Science. The images were viewed and analyzed using LSM710 Confocal Microscopy (Carl Zeiss) and ZEN 2009 software respectively. In all the statistical analyses, weighted colocalization coefficient was used.

2.19 Monoclonal Ab cross-competition analysis

To determine if the two anti-mDNase II mAbs #5-38 and #17 were derived from the same clone of hybridomas, Ba/F3 cells expressing mDNase II in pDisplay vector were pre-incubated with one of the undiluted mAb (unlabeled). The same or the other mAb

(biotinylated) was then added at the normal working concentration. Streptavidin-PE was used as the only secondary antibody bearing the fluorophore. The samples were then analyzed by flow cytometry.

2.20 Statistical method

Error bars in ELISA analysis were calculated according to the Student's *t* test.

3. Results

3.1 Role of DNase II in TLR9-mediated cytokine productions in BM-cDCs.

I first examined the requirement of DNase II in TLR9 responses in BM-cDCs, one of the major APCs, by stimulating with CpG-A or CpG-B at different doses. As a control, the cellular responses to the TLR4/MD-2 ligand, lipid A (the active ingredient of LPS), were also studied. Since the *Dnase2a*$^{-/-}$ mice die prenatally [58], I used the DNase II and type I IFN receptor double-deficient mice (*Dnase2a*$^{-/-}$*Ifnar1*$^{-/-}$) [59]. To ensure that the BM-cDCs obtained from the double-deficient mice differentiated normally after 1 week of culture with GM-CSF *in vitro*, the cells were stained with the surface markers CD11b and CD11c. The wildtype (WT), *Ifnar1*$^{-/-}$ and *Dnase2a*$^{-/-}$*Ifnar1*$^{-/-}$ BM-cDCs expressed similar percentage of CD11b and CD11c double positive cells after 1 week of culture (Figure 4a). I also examined TLR9 proteolytic cleavage in these cells, and found that both the full length and cleaved TLR9 fragments were similarly immunoprecipitated in the three genotypes observed (Figure 4b). Thus, the GM-CSF-induced BM-cDCs from the *Ifnar1*$^{-/-}$ and *Dnase2a*$^{-/-}$ *Ifnar1*$^{-/-}$ mice differentiated normally with similar expression levels of endogenous TLR9 as compared with the WT cells. Interestingly, when production of IL-12p40 and RANTES from the *Ifnar1*$^{-/-}$ and *Dnase2a*$^{-/-}$*Ifnar1*$^{-/-}$ BM-cDCs after CpG stimulation were measure with ELISA, only the CpG-A responses were severely impaired, while the CpG-B responses was mostly unaffected (Figure 4c).

In order to confirm the above observation in BM-cDCs that express intact IFN receptor 1, mice lacking DNase II specifically in hematopoietic cells were generated by mating *Dnase2a*$^{flox/flox}$ mice with *Tie2-Cre* transgenic mice. The conditional knockout mice generated (with genotype *Dnase2a*$^{flox/flox}$ *Tie2-Cre*) were analyzed.

Although the conditional knockout mice were born normally, the number of *Dnase2a*$^{flox/flox}$ *Tie2-Cre* mice obtained was much less than that predicted by the Mendelian ratio. The DNase II mRNA expression level was reduced by 80% in the mutant GM-CSF-induced BM-cDCs (Figure 4d upper panel). After a week of differentiation, the expression of CD11c and CD11b on the *Dnase2a*$^{flox/flox}$ *Tie2-Cre* BM-cDCs was similar to that of the *Dnase2a*$^{+/+}$ *Tie2-Cre* control (Figure 4d lower panel). Again, CpG-A response, but not CpG-B response, was impaired in the mutant BM-cDCs (Figure 4e). However, the drop in cytokine production was milder than that observed in *Dnase2a*$^{-/-}$*Ifnar1*$^{-/-}$ BM-cDCs, and this may be due to the residual DNase II expressed in these conditional knockout mice.

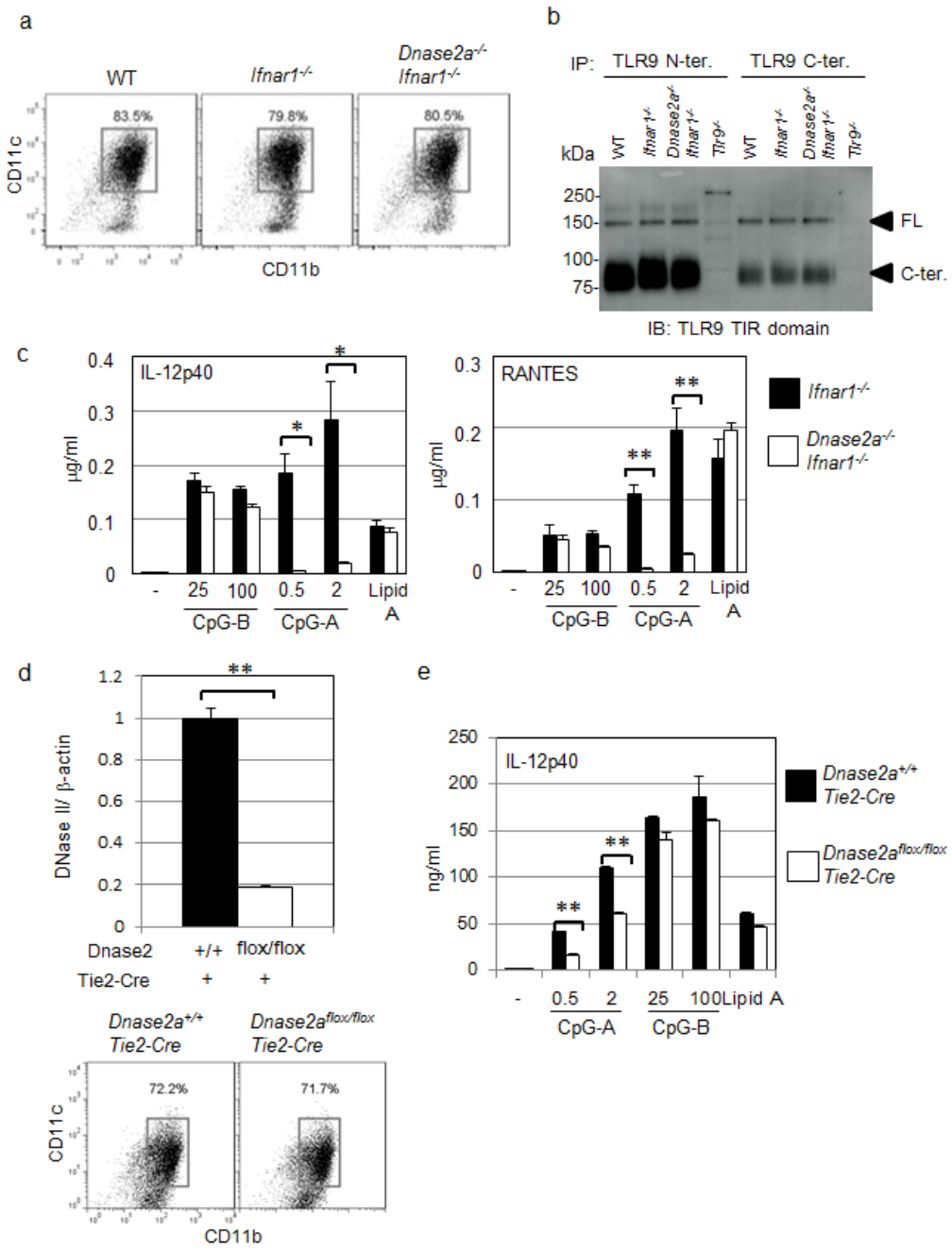

Figure 4. DNase II was only essential for CpG-A-induced TLR9 responses in BM-cDC. (a) Flow cytometry analysis showing the cell surface expression of CD11b and CD11c staining in the *in vitro* GM-CSF-derived BM-cDC obtained from WT, *Ifnar1*$^{-/-}$ or *Dnase2a*$^{-/-}$*Ifnar1*$^{-/-}$ mice. (b) Immunopreciptation of the endogenous TLR9 from the cells indicated. (c) Cell supernatants were collected 24 hours after ligand stimulations and cytokines productions were then measured by ELISA. (d) Real-time PCR analysis for checking the knockout efficiency in *Dnase2a*$^{flox/flox}$ *Tie2-Cre* GM-CSF-induced BM-cDCs. The surface expression of CD11b/CD11c on the BM-cDCs was analyzed by flow cytometry. (e) BM-cDCs from *Dnase2a*$^{flox/flox}$ *Tie2-Cre* mice were treated as in (c) and the IL-12p40 production measured by ELISA. The experiments in (a)-(c) were repeated for at least three times, while (d) and (e) were repeated twice due to unavailability of the conditional knockout mice. -, untreated. IP, immunopreciptation; IB, immunoblotting; N-ter., N-terminus; C-ter., C-terminus; FL, full length. *, $p<0.05$; **, $p<0.01$.

3.2 Impaired TLR9 responses in conditional DNase II-deficient BM-pDCs.

Since type I IFN signaling is important in pDCs in that positive feedback loop mediated by the type I IFN receptor is crucial for robust type I IFN response [73], the *Dnase2a*$^{flox/flox}$ *Tie2-Cre* mice were used to examine the responses of pDCs. The DNase II knockout efficiency in the Flt3 ligand-induced BM-pDCs was examined (Figure 5a). The DNase II mRNA expression was reduced but about 80% as determined by real-time PCR. The surface CD11c and B220 expressions were also comparable in both the control and *Dnase2a*$^{flox/flox}$ *Tie2-Cre* BM-pDCs (Figure 5b). The gated cells shown in Figure 5b were sorted and used in the following experiments. To examine the TLR9 responses in the DNase II-deficient BM-pDCs, the cells were treated with CpG-A or CpG-B and cytokine production was evaluated by ELISA. IL-12p40 secretion was impaired upon CpG-A stimulation (Figure 5c). The IFN-α production was also measured after CpG-A stimulation. As expected, CpG-A-induced IFN-α production was significantly diminished in the BM-pDCs (Figure 5d). In both IL-12p40 and IFN-α, the reductions were not as dramatic as those found in BM-cDCs (Figure 4). Such difference maybe due to the incomplete ablation of DNase II in these pDCs. Thus, together with the results from BM-cDCs, TLR9 signaling requires DNase II in order to mount an intact response especially towards one of its ligands, CpG-A.

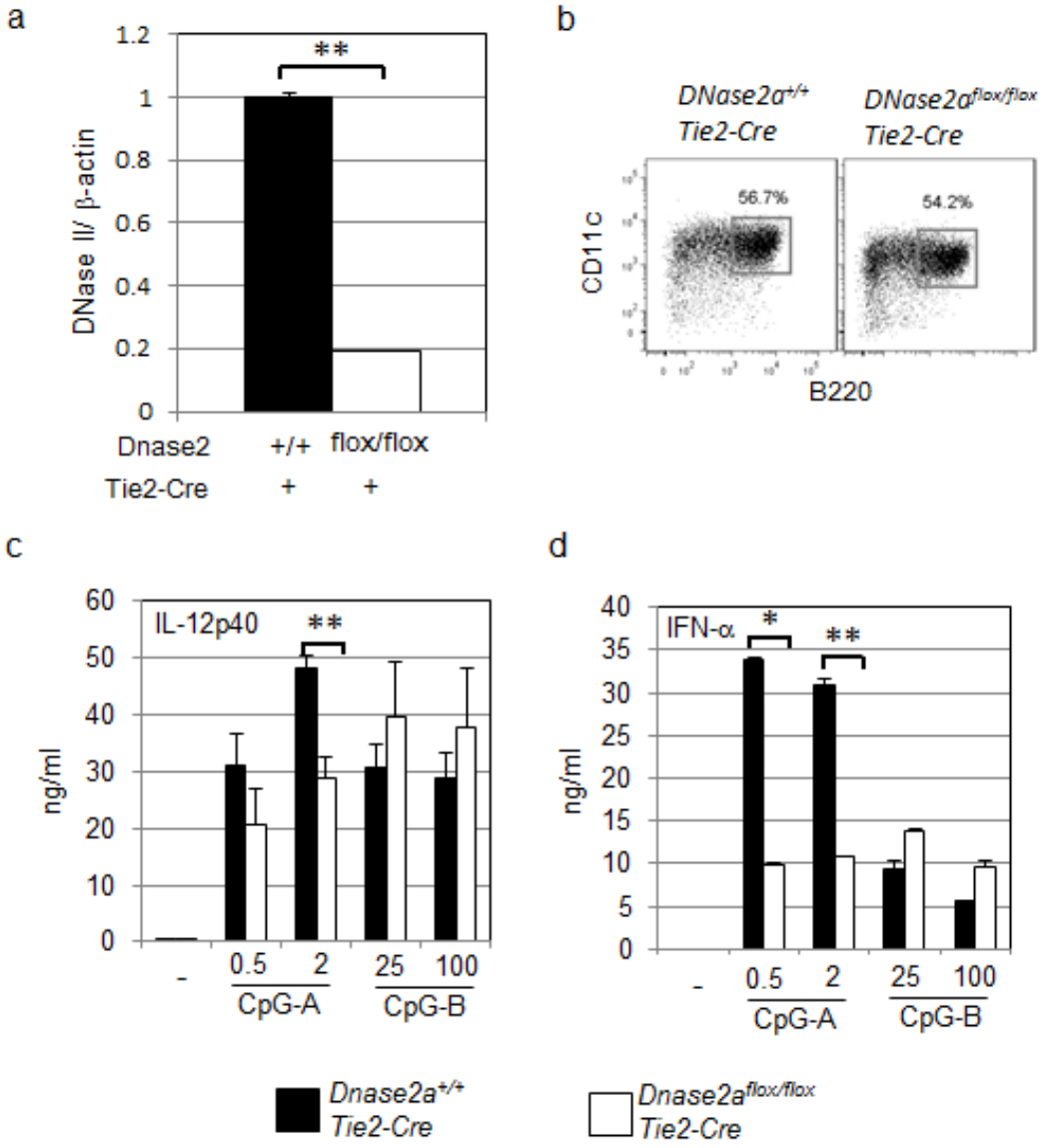

Figure 5. CpG-A responses required the presence of DNase II in BM-pDCs. (a) About 80% of DNase II was reduced in the *Dnase2a*$^{flox/flox}$ *Tie2-Cre* BM-pDCs as determined by quantitative real-time PCR. (b) The gated population of the Flt3L-induced pDCs were sorted and used in experiments. (c) ELISA detection of IL-12p40 or IFN-α production after stimulation of the sorted cells from (b) with various doses of CpG-B (nM) or CpG-A (μM) for 24 hours. The experiments were only repeated twice as only two *Dnase2a*$^{flox/flox}$ *Tie2-Cre* mice were available for analysis. *, $p<0.05$; **, $p<0.01$.

3.3 Effect of DNase II-deficiency on CpG ODNs uptake in BM-cDCs

To investigate the step where DNase II exerted its effect on TLR9 responses, possible defect in DNA internalization in *Dnase2a*$^{-/-}$*Ifnar1*$^{-/-}$ BM-cDCs was examined. FITC-labeled CpG-A or CpG-B was incubated with the BM-cDCs. After incubation, fluorescence by the surface-bound CpG ODN was removed by quenching. The fluorescent CpG ODN remained inside the cells after internalization was examined by flow cytometry analysis.

The amount of fluorescent CpG-A or CpG-B internalized by the cells was not differ between the *Ifnar1*$^{-/-}$ and *Dnase2a*$^{-/-}$ *Ifnar1*$^{-/-}$ BM-cDCs 30 or 120 minutes after incubation (Figure 6). This indicated that DNase II is not required for DNA uptake and subsequent internalization in BM-cDCs.

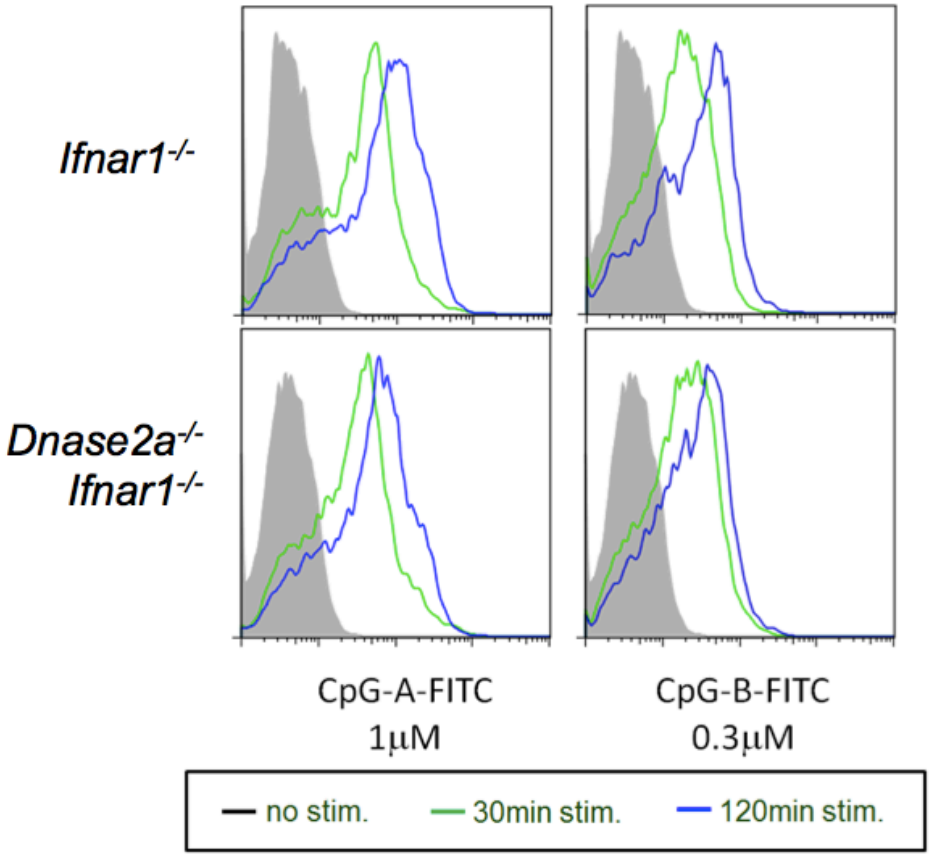

Figure 6. DNase II did not affect CpG ODN uptake in BM-cDCs. The cells were incubated with the FITC-conjugated CpG ODN for 30 or 120 minutes at 37°C and quenched before flow cytometry analysis. A representative result out of 3 trials is shown.

3.4 Requirement of the enzymatic activity of DNase II for TLR9 responses.

To gain a mechanistic insight into the role of DNase II in CpG-A responses, the requirement for the DNase activity was examined. Histidines at the amino acid positions 115, 132, and 297 are indispensable for DNase activity in porcine DNase II, and these three sites are conserved in the murine homolog (Figure 7). It was also shown that the H132A DNase II mutant is trapped in the ER and cannot be secreted, implying that the histidine at amino acid position 132 is important for proper protein folding [74].

In this study, I constructed the H115A and H297A mutants, containing Alanine in lieu of Histidine at position 115 or 297 respectively. The H115A and H297A mutants were overexpressed separately in cell line and purified (Figure 8a). It is noticed that the H115A and H297A mutants exhibits a higher apparent molecular weight compared with the WT protein, presumably owing to an additional glycosylation on these mutants [74]. The DNase activities of these mutants were evaluated by incubation with plasmid DNA. H297A DNase II failed to degrade DNA even after 24 hours of incubation (Figure 8b), indicating that the mutant is enzymatically inactive. However, the H115A mutant still remained residual activity as shown by after 24 hours of incubation using a higher dose of the protein.

Next, the ability of the H297A mutant to rescue the TLR9 responses upon CpG-A stimulation in the DNase II-deficient cells was monitored. Green fluorescent protein (GFP)-tagged WT or H297A DNase II was transduced into the bone marrow stem cell obtained from the *Dnase2a*$^{-/-}$*Ifnar1*$^{-/-}$ mice. The cells were allowed to differentiate into cDC in the presence of GM-CSF. Flow cytrometry analysis showed that the transduction efficiencies were similar between the WT and the H297A mutant (Figure 8c). These transduced cDCs were subjected to stimulation with CpG-A and

cytokine production examined. Only the WT DNase II was able to rescue the TLR9 responses to CpG-A, but not the enzymatically-deficient mutant H297A (Figure 8d). From these results, I conclude that the enzymatic activity of DNase II is required for the TLR9 signaling by CpG-A.

a

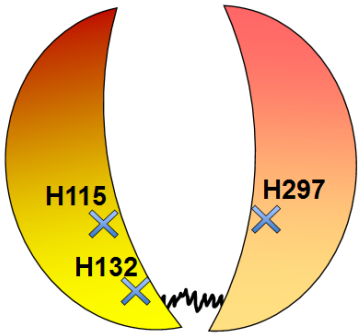

b

MATLRSLLLAALLWVPAEALSCYGDSGQPVDWFVVYKLPAHSGSRDTPKGLTYKYMDQNSDGWQD
GVGYINSSEGAVGRSLQPLYRKNSSQLAFLLYNDQPPKSSSARDSTGHG**H**TKGVLLLDQEGGFWLV**H**S
VPRFPPPASSGAYTWPPNAQTFGQTLLCVSLPFTQFARIGKQLTY*TYPLVYDHKLEGFFAQKLPDLETVI*
*KNQHVLH*EPWNSSVILTSQAGATFQSFAKFGKFGDDLYSGWLAEALGTNLQVQFWQNSPGILPSNC
SGAYQVLDVTQTGFPGPSRLTFSATED**H**SKWCVAPQGPWACVGDMNRNKAETHRGGGTVCTQLPS
FWKAFQSLVKDWKPCIEGS

Figure 7. Schematic representation of the murine WT DNase II and its amino acid sequence. (a) Native mouse DNase II is predicted to be composed of one single polypeptide with two symmetric motifs. The three histidine (H) residues critical for enzymatic activity are denoted by a cross with amino acid positions written. (b) Amino acid sequence of the mouse *Dnase2a*. The letters in red are the histidine residues marked in (a). The sequence in green is the amino acids linking the two putative halves of the enzyme.

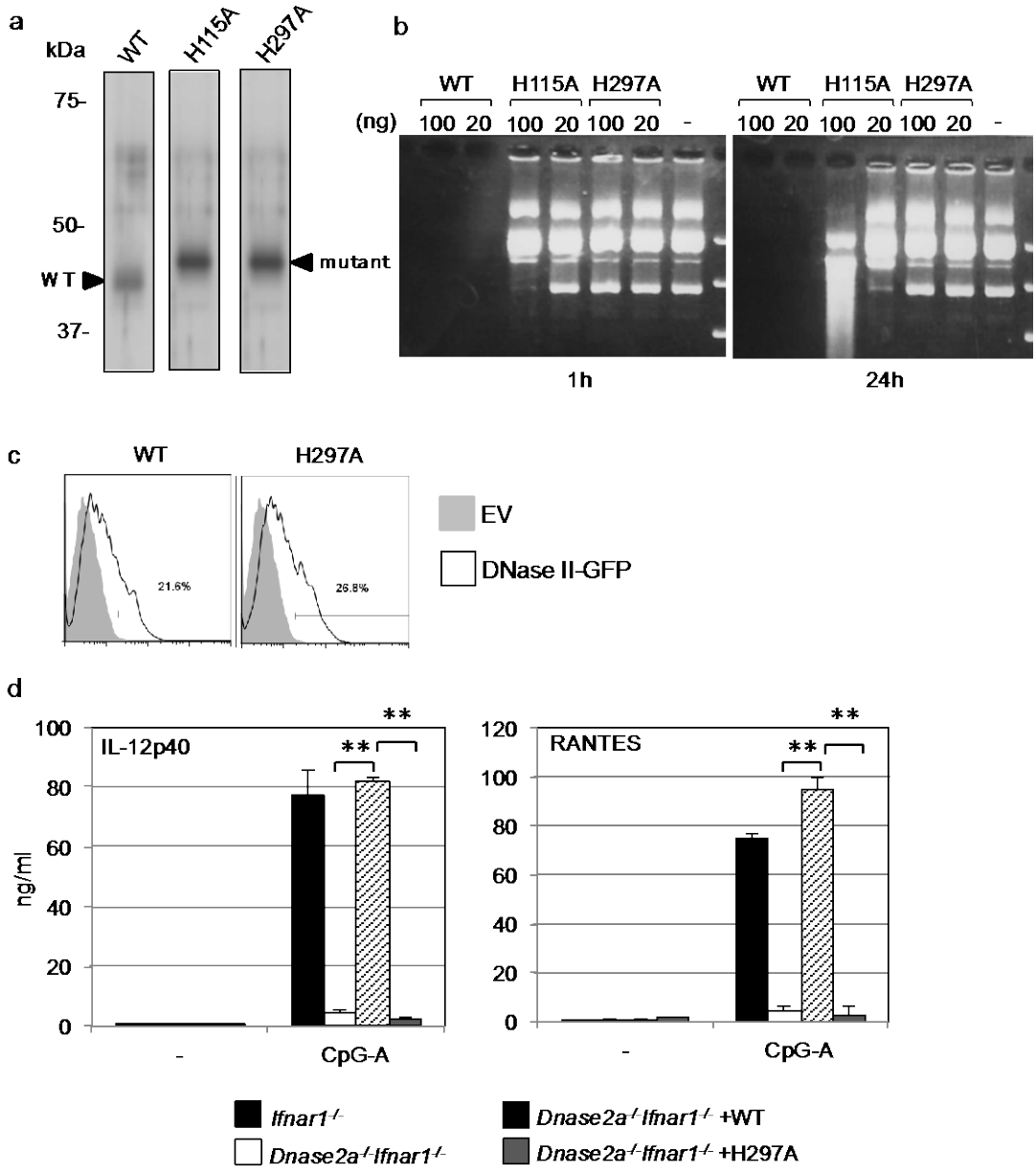

Figure 8. Only the enzymatically active WT DNase II was able to complement the TLR9 responses in the *Dnase2a*$^{-/-}$*Ifnar1*$^{-/-}$ BM stem cell cDCs. (a) The WT, H115A or H297A DNase II was allowed to express in a cell line and the secreted DNase II was purified and visualized by silver staining (The bands were cut out since the proteins were not run in adjacent lanes, although they were run on the same polyacrylamide gel). (b) Activities of the purified proteins were examined by DNA digestion assay for 1 hour or 24 hours as shown. (c) WT or the H297A mutant DNase II was transduced into the cells, and the transduction efficiencies determined by flow cytometry analysis. (d) The transduced BM-cDCs were stimulated with 1.5μM of CpG-A for 24 hours. IL-12p40 or RANTES secretions in the culture supernatant were measured by ELISA. EV, empty vector. Each set of experiment was repeated for three times. **, $p<0.01$.

3.5 Cleavage of CpG-A by DNase II.

Since the expression of enzymatically active DNase II but not inactive DNase II rescued TLR9 responses to CpG-A in DNase II-deficient cells, it is possible that CpG-A is cleaved by DNase II. Using the purified DNase II proteins as shown in Figure 8a, I next performed *in vitro* DNA cleavage experiments. The CpG-A that was used throughout this study consists of 20 nucleotides. After 24 hours of incubation with different doses of WT or mutant DNase II, a shorter band of DNA was observed only in incubating with the WT DNase II (indicated by black arrow in Figure 9a), but not with the H115A or H297A mutant. Such cleavage was not observed in case of CpG-B. From these results, it is speculated that the major role of DNase II is to cut CpG-A into smaller pieces, which may directly stimulate TLR9.

To mimic the cleaved CpG-A, truncated CpG-A 2216 fragments of various lengths were synthesized based on the original sequence (Figure 9b). CpG-A-like ODNs containing the 5'-9 or -11 nucleotides, or the 3'-9, -10, -11, -12 bases of the original sequences were designed. Comparing the DNase II-cleaved CpG-A (indicated by white arrow in Figure 9c) and the 9-12-nucleotide fragments, I observed that the cleaved band of CpG-A had a length of around 11 bases (Figure 9c). To confirm that these CpG-A fragments specifically activated TLR9, BM-cDC response from the *Tlr9*$^{-/-}$ mice was examined. Among the four types of short CpG-A examined, only the A3'11 ODN induced a detectable amount of IL-12p40 from the WT BM-cDC, but not from *Tlr9*$^{-/-}$ BM-cDC (Figure 9d). Although the short CpG-A alone was stimulatory to the WT cells, complexing with the transfection reagent, lipofectamine, enhanced TLR9 activation by the short CpG-A fragment, which was also TLR9-dependent (Figure 9d). To investigate the requirement of DNase II in TLR9 activation by these short CpG-A ODNs, BM-cDCs from the *Dnase2a*$^{-/-}$*Ifnar1*$^{-/-}$ mice were

treated similarly as in Figure 9d. The results showed that the *Dnase2a*$^{-/-}$*Ifnar1*$^{-/-}$ BM-cDCs responded to the truncated CpG-A fragment A3'11 ODN by producing as much cytokine as the *Ifnar1*$^{-/-}$ control cells (Figure 9e). The same results were obtained with or without the addition of lipofectamine.

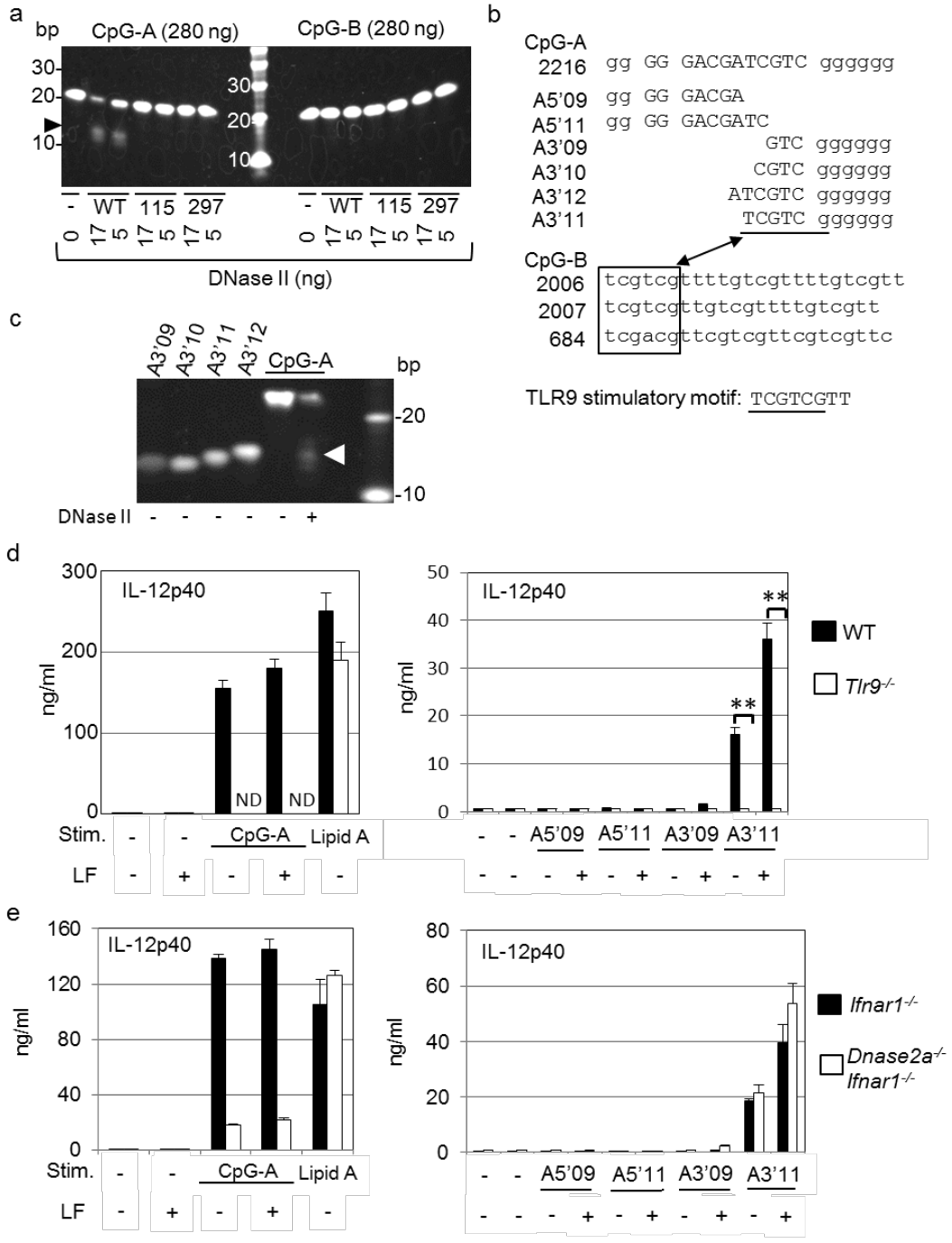

Figure 9. A truncated CpG-A sequence stimulated TLR9 in BM-cDCs even in the absence of DNase II. (a) WT DNase II was shown to cleave CpG-A from a 20-base sequence to about 10 bases (pointed by black arrow). (b) Short CpG-A fragments based on the original CpG-A ODN 2216 were synthesized. Compare with several CpG-B sequences shown, the A3'11mer has sequence (underlined) similar to the 5'-6 bases in CpG-B (boxed). (c) DNase II-cleaved CpG-A (pointed by white arrow) was run in parallel with several truncated CpG-A fragments of various lengths. (d) TLR9-dependency of some of the fragments shown in (b) was examined. (e) The responses of the *Dnase2a*$^{-/-}$*Ifnar1*$^{-/-}$ BM-cDCs towards the short CpG-A ODNs were measured by ELISA. All the experiments shown had been repeated for three times. Stim., stimulation; LF, lipofectamine. **, $p<0.01$.

3.6 Generation of monoclonal antibodies against endogenous DNase II

Identifying the distribution of endogenous DNase II is important in understanding its mechanism of action. As monoclonal antibody (mAb) against mouse DNase II was not available, it was generated by immunizing *Dnase2a*$^{-/-}$*Ifnar1*$^{-/-}$ mouse with the purified mouse WT DNase II protein as shown in Figure 8a. Two positive monoclones (#5-38 and #17) were obtained after screening. The mAbs were typed as IgG1 with kappa light chain (Figure 10).

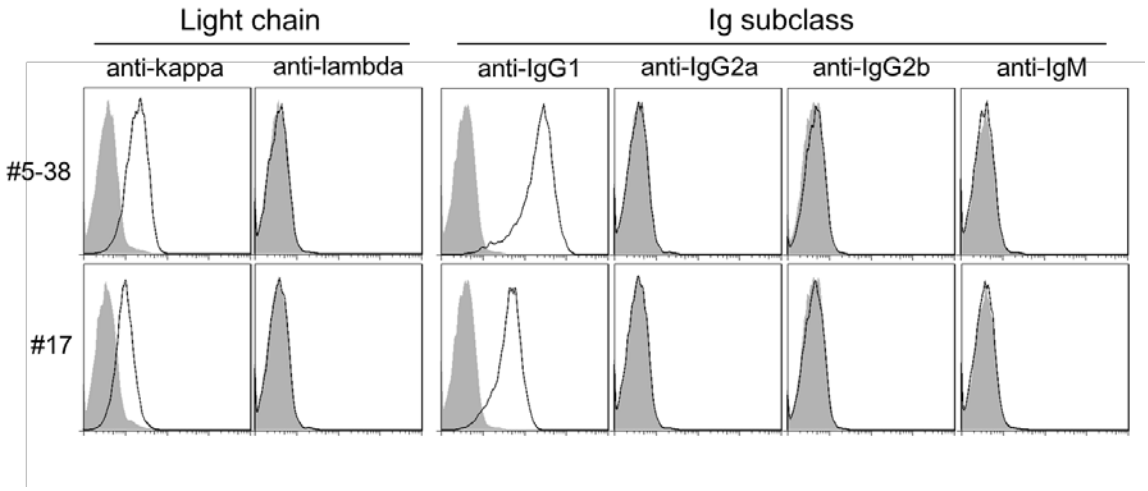

Figure 10. Characterization of the anti-mDNase II mAbs established. The type of light chain and the Ig subclasses of the two monoclones were examined by flow cytometry analysis using Ba/F3 cells overexpressing the WT DNase II on the cell surface.

Next, to determine the usability and specificity of these mAbs, they were tested in immunoprecipitation and confocal microscopy experiments, with the *Dnase2a*$^{-/-}$*Ifnar1*$^{-/-}$ BM-cDCs used as the negative control (Figure 11). As pre-incubating one mAb was unable to block the staining using the other mAb, they were regarded as targeting different DNase II epitopes (Figure 11a). Both sepharose-conjugated #5-38 and #17 were capable of immunoprecipitating the endogenous DNase II in WT, *Tlr9*$^{-/-}$ and *Ifnar1*$^{-/-}$ BM-cDCs, but not from *Dnase2a*$^{-/-}$*Ifnar1*$^{-/-}$ cDCs (Figure 11b). For confocal microscopy, using the same staining conditions, #17 stained the endogenous DNase II more efficiently than the #5-38 mAb (Figure 11c). Thus, #17 was used in subsequent confocal experiments. The DNase II staining in WT BM-cDCs using mAb #17 were also shown (Figure 11c).

In addition to detecting WT DNase II, the mAbs also recognized the H115A and H297A mutants, but not the H132A mutant (Figure 12). These results showed that single amino acid mutations in the H115A and H297A mutants did not affect the antibody-binding epitopes for both mAbs.

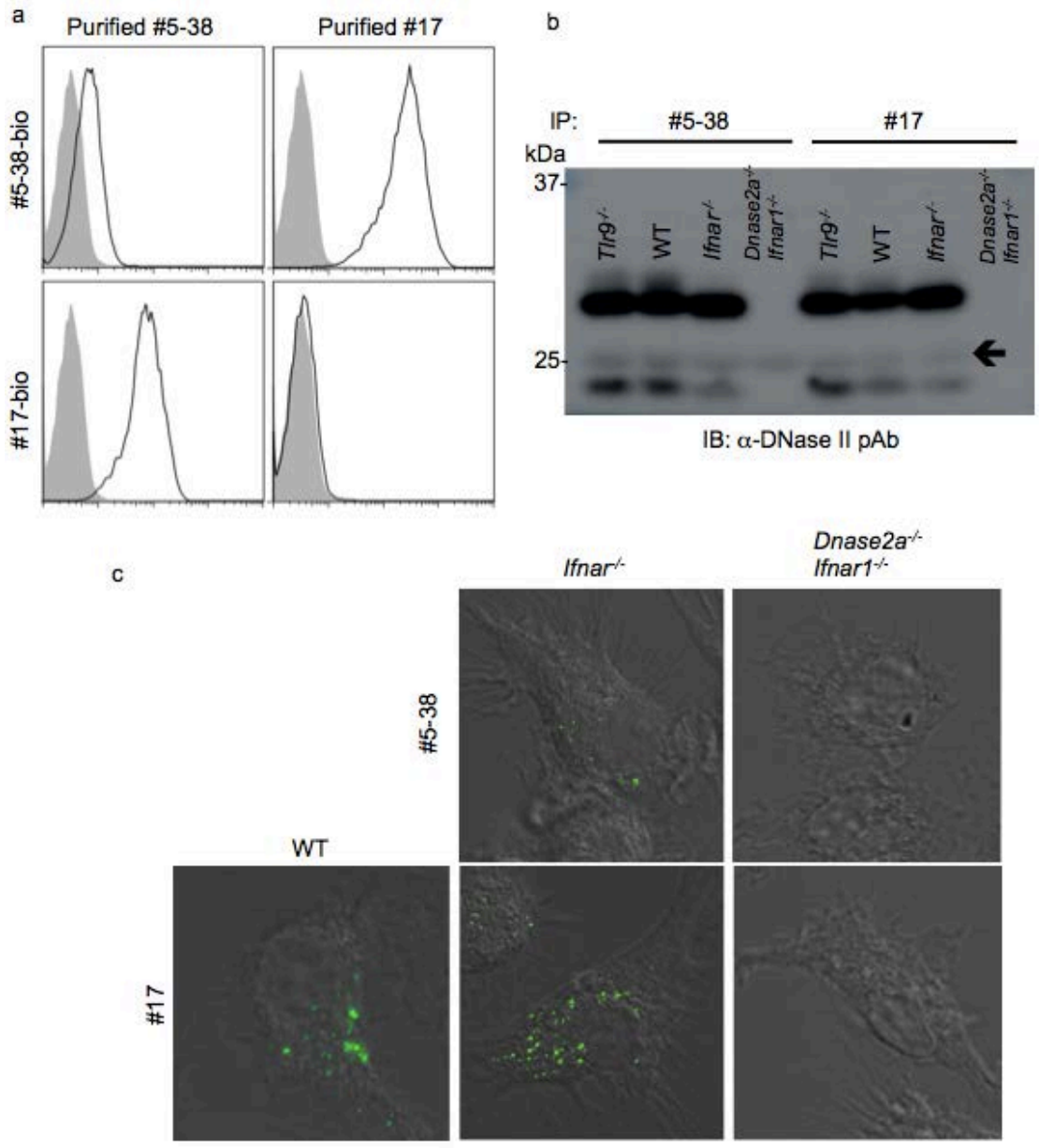

Figure 11. The anti-mDNase II mAbs detected different epitopes and were applicable to immunoprecipitation and confocal experiments for detecting the endogenous DNase II protein. (a) Cross-competition analysis using Ba/F3 cells overexpressing DNase II anchored on the cell surface via the pDisplay vector. Streptavidin-PE was used as the secondary antibody before flow cytometry analysis. (b) BM-cDCs were lysed and the endogenous DNase II was immunopreciptated by either mAb in all the three genotypes shown, but not in *Dnase2a*$^{-/-}$*Ifnar1*$^{-/-}$ cDCs. The arrow represent non-specific signal. (c) Confocal staining of endogenous DNase II in BM-cDCs using the two mAbs.

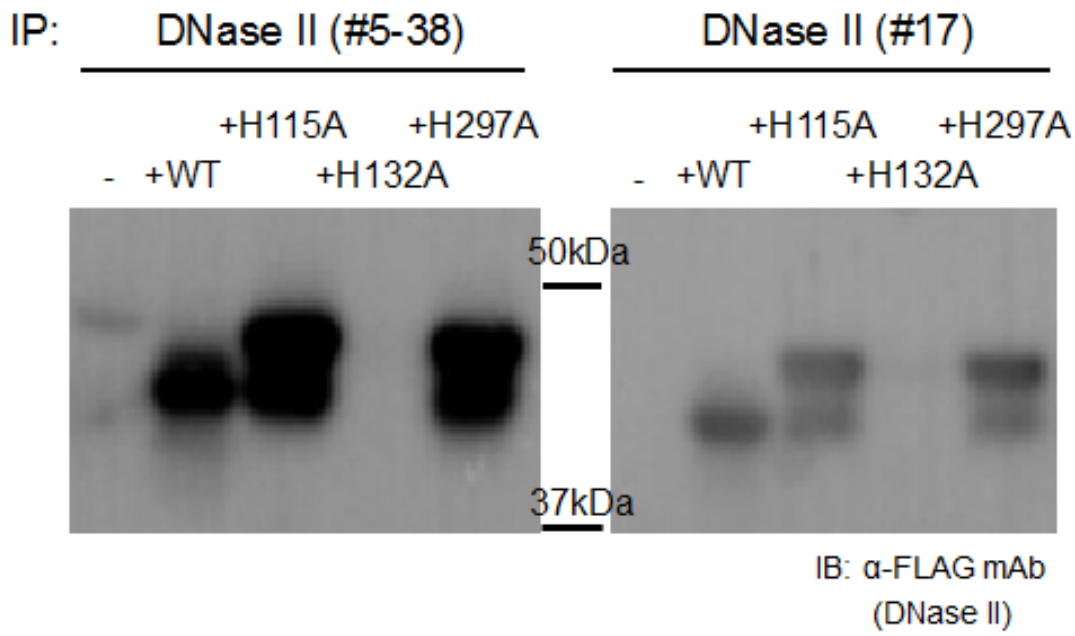

Figure 12. The mAbs recognized the WT, H115A and H297A, but not H132A DNase II. Ba/F3 cells were transduced with the indicated constructs (each with a FLAG-His tag at the 3' end). The respective cell lysates were collected and immunoprecipiated with the respective anti-DNase II mAbs. The membranes after Western blotting were immunoblotted with anti-FLAG M2 mAb, and detected using the ECL system.

3.7 CpG-A induced lysosomal trafficking of DNase II.

The results obtained from previous sections suggest that TLR9 requires DNase II-dependent CpG-A cleavage, but not for CpG-B. Since the optimal environment of DNase II activity is below pH5.6 [75], it is speculated that DNase II would colocalize with CpG-A in acidic compartment, such as the lysosome.

The steady state subcellular localization of DNase II was first determined with the mAb #17. It is believed that DNase II mainly resides in the lysosome in the resting state [68]. Using the established mAbs to detect the endogenous DNase II, it was observed that a significant amount of DNase II resided in the lysosomes (stained with the lysosome-associated membrane protein 1 (LAMP1) or LAMP2) than the ER or early endosome (stained with calnexin and early endosome-associated protein 1, EEA1, respectively). However, even greater amount of DNase II was found to colocalize with the lectin wheat germ agglutinin (WGA) (Figure 13a).

Localization of DNase II after CpG-A, CpG-B or the A3'11 ODN treatment was then studied. At 3, 6 and 8 hours after addition of the respective CpG ODN, the WT BM-cDCs were fixed and stained with the endogenous DNase II and the lysosome marker LAMP2 for confocal analysis. CpG-A induced increasing colocalization of DNase II with LAMP2 (Figure 13b), whereas CpG-B did not recruit DNase II to the lysosome for the same time courses examined (Figure 13c). Similarly, the A3'11 ODN, which may resemble the DNase II-processed CpG-A (Figure 9), also did not affect the localization of DNase II with LAMP2 (Figure 13d). Fluorescent CpG-A was also found in LAMP2-positive compartment after 8 hours (Figure 13e). This is in contrast to that of CpG-B or the A3'11 ODN.

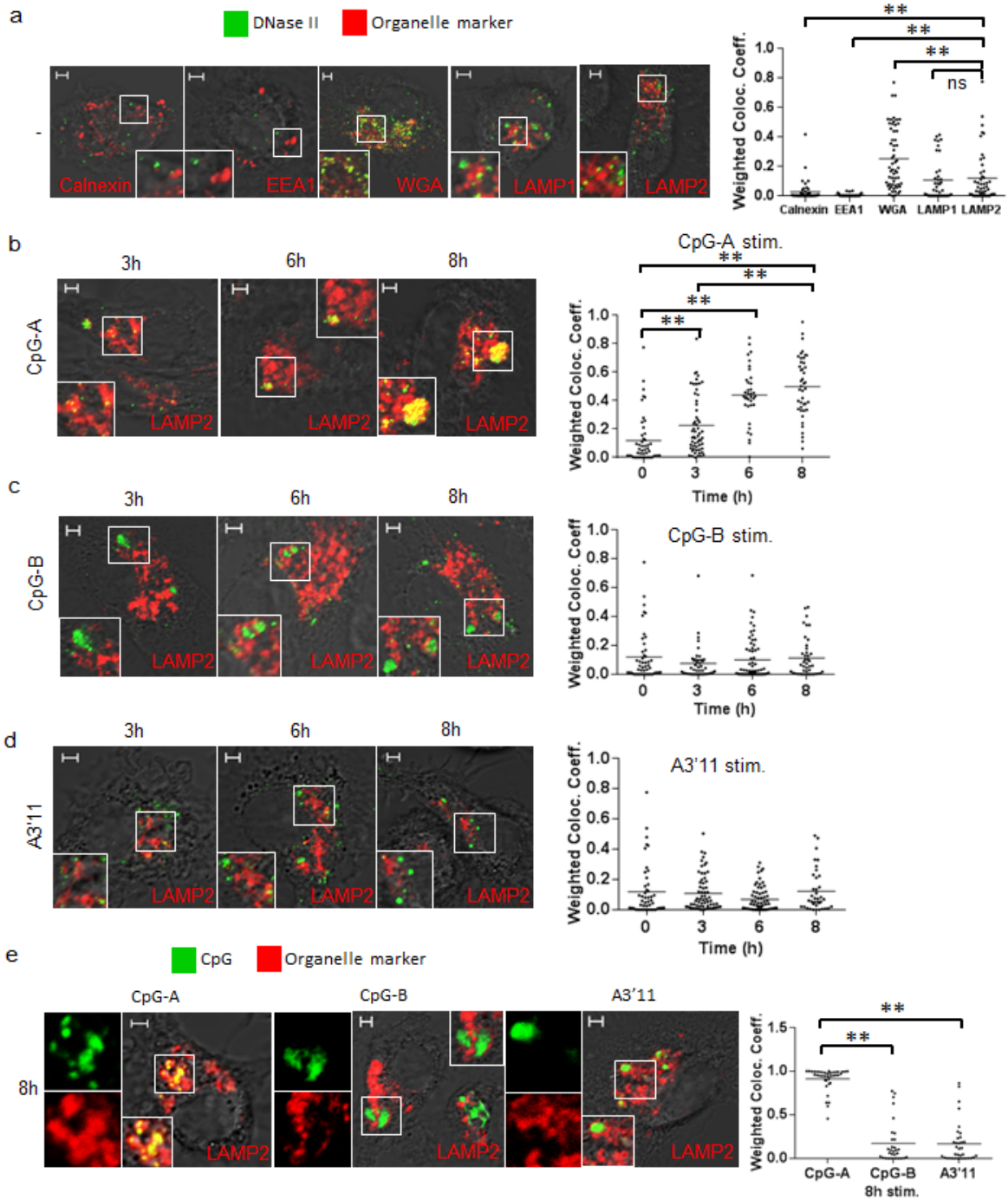

Figure 13. Localization of the endogenous DNase II in resting and stimulated states in WT BM-cDCs. (a) Double staining of DNase II and various organelle markers in the resting state. DNase II and LAMP2 were stained in stimulated cells after 3, 6 or 8 hours, 1.5μM of each of the (b) CpG-A, (c) CpG-B or (d) the ODN A3'11 were used. (e) Localizations of CpG-A, CpG-B or A3'11 ODN were monitored by staining with LAMP2 8 hours after addition. DNase II and various organelle markers were indicated as green and red fluorescence respectively in (a-d). In (e), green represents ODNs, while red represents LAMP2. All the experiments have been repeated for at least three independent trials. Scale bar at the left upper corners represents 2μm; ns, not significant; *, $p<0.05$; **, $p<0.01$.

4. Discussion

4.1 Putative stimulatory motif for TLR9 activation

The present study demonstrated that DNase II was required for TLR9-mediated responses to CpG-A, but not to another ligand of TLR9, CpG-B. Such observation was consistently found in both BM-cDC (from the *Dnase2a*$^{-/-}$*Ifnar1*$^{-/-}$ and *Dnase2a*$^{flox/flox}$ *Tie2-Cre* mice) and BM-pDC (from the *Dnase2a*$^{flox/flox}$ *Tie2-Cre* mice). Further examination revealed that the active sites in H115 and H297 of the murine DNase II were indispensable in supporting the TLR9 responses. Re-introduction of WT DNase II rendered the *Dnase2a*$^{-/-}$*Ifnar1*$^{-/-}$ cDCs responsive to CpG-A stimulation. This led to the finding that CpG-A was indeed cleaved by the WT DNase II. Although I have not examined whether the cleaved product of CpG-A by the WT DNase II can stimulate TLR9 in this study, the synthetic short CpG-A-like ODNs (A3'11 ODN) with similar length with the cleaved product (about 11 bases as judged in the TBE gel electrophoresis) was made, and found to induce the cytokine production response in the DNase II-deficient BM-cDCs. It is interesting that out of the 4 types of short CpG-A examined (A5'09, A5'11, A3'09, A3'11), only A3'11 was able to induce similar amount of cytokine in *Ifnar1*$^{-/-}$ and *Dnase2a*$^{-/-}$*Ifnar1*$^{-/-}$ BM-cDCs. It has been reported that CpG ODN sequence of GTCGTT is potent in stimulating cells from various species, and that when such sequence is preceded by a TC dinucleotide, the stimulating effect is even more prominent [27]. With referring to the underlined sequence in Figure 9b, the A3'11 ODN contains the first 4 nucleotides (GTCG) in the GTCGTT sequence, with a TC dinucleotide in front of GTCG. Only TCGTCG may also be able to stimulate TLR9. The combination of TC and GTCG was not found in the other three sequences studied (A5'09, A5'11, A3'09). Thus, the role of DNase II-

dependent cleavage of CpG-A may be just to expose such motif to stimulate TLR9. Consistent with this notion, CpG-containing sequences as short as 5-6 nucleotides in length are enough to stimulate the human and murine DCs [76, 77]. On the contrary to CpG-A, CpG-B responses were not dependent on DNase II, and it was not cleaved by incubation with DNase II. Apart from the DNase-resistance in the phosphorothioated backbone, this may be explained by the fact that the first several bases found in the CpG-B matches the "TC+GTCG" pattern as described above, therefore are sufficient in directly stimulating TLR9. Some of the CpG-B sequences used to stimulate TLR9 also harbor sequence that is similar to the first couples of nucleotides found in the A3'11 ODN. However, even though the A3'11 ODN can stimulate TLR9 in the absence of DNase II, it does not necessarily represent the real cleaved product of CpG-A by DNase II. The exact sequence may be determined by purifying the cleaved product and subcloned into plasmid vector for sequencing.

4.2 Localization of DNase II in resting and stimulated states

Since mAb against the endogenous murine DNase II is not currently available, I generated them in this study. With the mAb, the subcellular distribution of DNase II in BM-cDCs was studied. The results show that in addition to lysosome-localization as reported, DNase II also resided in compartments stained with the lectin WGA. Compared with the colocalization observed with WGA, only a fraction of DNase II was localized in LAMP1/LAMP2-positive lysosome, but not with calnexin or EEA1 in BM-cDC. A recent report has shown that DNase II is localized in LAMP1 positive lysosome in cyrosections of the murine spleen and bone marrow, using a polyclonal anti-DNase II antibody they have generated [78]. However, from their results, the LAMP1-stained region was mainly surrounding albeit with very partial apparent

colocalization, with DNase II. Thus, it is possible that most of the DNase II is not found in lysosomes but other compartments. Wheat germ agglutinin (WGA) has been shown to specifically stain the *trans*-Golgi subcompartment [79, 80]. However, in another study, the authors compare the reliability of WGA on staining the Golgi apparatus before and after treatment with a cytokinesis inhibitor. They found that WGA overlaps with the *trans*-Golgi markers, the *trans*-Golgi network 46 (TGN46), but not with another *trans*-Golgi markers, syntaxin-6 [81]. Thus, it implies that WGA staining does not necessarily represent the Golgi apparatus in all the cell status or cell types. The murine DNase II has a calculated molecule weight of about 35kDa based on the transcript length. It is believed to be cleaved from the pro-enzyme to two products of 30-35 and 10-23kDa [74, 78] by cathepsins [78]. Consistent with this, our results also demonstrated that the endogenous DNase II in BM-cDCs was cleaved into two products of around 30 and 23 kDa. During the proteolytic processing, some of the DNase II proteins may remain and function at the Golgi apparatus, while some are being transported to lysosome. It would be interesting to discriminate which pool(s) of DNase II is/are important in facilitating the responses of TLR9 upon CpG-A stimulation.

Our results have shown that in BM-cDC, after CpG-A stimulation, DNase II was progressively recruited into LAMP2-positive lysosomal compartments. Besides, nearly all of the CpG-A was found in such LAMP2-positive lysosome 8 hours after stimulation. This is consistent with earlier study that in cDC, CpG-A preferentially moves to the LysoTracker-stained lysosome, in contrast to the endosomal retention found in pDC [52]. However, different from the previous study [52], we observed that CpG-B was mostly localized outside the lysosomes, albeit very close to the LAMP2-stained compartment. Other study also shows that CpG-B DNA localizes in

lysosomes in pDCs [82]. Although additional reports show the same results, the type of CpG ODN used in the localization analysis is not specified [83, 84]. One of the possible explanations for the discrepancy in the current and previous studies is that, there are different kinds of lysosomes, which may be characterized by different sets of markers. LAMP2 used in the current study may not represent all the LysoTracker-positive lysosomes exist in cDCs.

Since CpG-A is potent in inducing type I IFN [29], and that IFN induction by TLR9 requires trafficking to lysosome-related organelle, which is also characterized by LAMP2 [69], DNase II may cleave CpG-A into short sequences in the lysosome, which in turn activate TLR9 to produce IFN in BM-cDCs. In case of BM-pDCs, as CpG-A is retained inside the endosome for type I IFN induction [52], and that DNase II is required for type I IFN production by CpG-A as found in this study, DNase II may be recruited to the endosome to cleave CpG-A in BM-pDCs, instead of the lysosome. The pH of the endosome where CpG-A is localized in BM-pDCs may be acidic enough for DNase II activity.

4.3 Property of DNA ligands that induce DNase II intracellular trafficking

From the confocal analysis, I have shown that CpG-B and A3'11 ODN did not induce lysosome trafficking of DNase II. This implies that for DNA that needs not to be cleaved, DNase II would not respond or move to lysosomes. Whether a DNA fragment has to be cleaved or not is likely to depend on its ability to form nanoparticles inside the cell. It may be DNA nanoparticle that recruits DNase II. Previous study has shown that in pDCs, the multimeric nature of the CpG-A ODN, rather than its sequence, is responsible for potent IFN-α production mediated by TLR9 [32, 85]. Multimerization of ODN can be achieved by using its 3' poly-G

extension or by complexing with the cationic lipid *N*-[1-(2,3-dioleoyloxy)]-*N*,*N*,*N*-trimethylammoniumpropan methylsulphate (DOTAP) [52, 85]. The DNA/cationic lipid complex has been suggested to mimic virus that carries its genetic materials across the cell membrane [86]. In this regard, self-DNA also can stimulate TLR9 by complexing with endogenous DNA-binding proteins for type I IFN release. In psoriasis, an autoimmune lesion of the skin, DNA that is released from skin cell injury is captured by the anti-microbial peptide LL37 (also known as cathelicidin antimicrobial peptide, CAMP). The DNA/LL37 complex stimulates pDCs to produce IFN-α via TLR9, ultimately breaking the innate tolerance and trigger the disease [87, 88]. Besides, LL37 is also important in carrying the DNA/antibody complex in SLE patients so as to prevent the complex from nuclease degradation [89]. Similarly, high-mobility group box (HMGB) proteins, the nuclear DNA-binding proteins, can also bind to DNA or CpG ODNs to promote internalization into pDCs, and activates TLR9 and cytosolic DNA sensors to produce IFN-α [90, 91]. Taking into account the role of DNase II in activating TLR9 for IFN-α production, the protein carriers (LL37 or HMGBs) binding to self-DNA or CpG ODNs may facilitate DNA contact, acting as a catalyst to speed up the DNA-cleaving reaction mediated by DNase II. It would be interesting to examine any interaction between these carriers and DNase II in the context of TLR9-dependent autoimmune diseases like psoriasis and SLE.

How the DNA nanoparticles activate cellular machinery or DNase II is still unknown. However, from the confocal microscopy results, it is known that in the resting state, more of the DNase II proteins may remain in the Golgi apparatus, presumably in the TGN, instead of the lysosome. Therefore, it is possible that the CpG-A nanoparticles have engaged the retrograde transport pathway, and are being carried from the endosome to the TGN [92]. At the TGN, numerous DNase II proteins

may bind to a CpG-A nanoparticle due to its large size compared with CpG-B or A3'11 ODN. The protein machinery for multivesicular bodies/lysosome biogenesis, the endosomal sorting complex required for transport (ESCRT) [93], may be able to sense or interact with DNase II/CpG-A complex, so as to direct vesicle fusion with lysosome. Thus, it is interesting to examine any interaction between the ESCRT subunits with DNase II after CpG-A stimulation.

4.4 Possible explanation for the anergy of TLR9 in DNase II single-knockout mice model

Kawane and others have reported in their series of studies that single knockout of DNase II in mice is embryonically lethal due to the induction of various defects [57-59, 62, 94]. Later, it is found that the cytosolic DNA sensor/adaptor STING is responsible for the excessive production of IFN-β that finally kills the organism [56]. The results presented in this study suggest that TLR9 may only be able to recognize DNA that are cleaved by DNase II and contains a stimulatory motif to induce IFN. The apoptotic DNA that is accumulated would not be able to trigger TLR9, since it is too long and the stimulatory sequence may not be exposed to TLR9. The accumulated DNA possibly leaks into the cytoplasm and activates STING. The type of DNA ligands that is recognized by STING may be less restricted compared with the DNA that stimulates TLR9. STING detects a wide variety of DNA ranging from necrotic or apoptotic DNA to single-stranded or double-stranded DNA-containing pathogens [95]. Recent studies found that STING is activated by the upstream second messenger, cGAMP, which is generated by cGAS [9, 10, 96]. In the DNase II single knockout mice model, the DNase II-TLR9 pathway for IFN induction is impaired while the cGAS-STING pathway remains intact and functional. This may mean that STING can

fully respond to cGAS-generated ligands, whereas TLR9 is not fully functional because the enzyme (DNase II) that produces TLR9 ligands (likely to be cleaved short DNA fragment) is ablated. Consequentially, there seems to have a certain degree of crosstalk between the cGAS-STING pathway and the DNase II-TLR9 pathway, because STING activity is also controlled by DNase II [95]. It is intriguing to know if knockout of cGAS would affect TLR9 responses.

4.5 Potential therapeutic application of the current findings

As mentioned in the Introduction, DNase II is required to digest apoptotic DNA in mice [57]. Together with the results obtained in the current study, DNase II may have a role in inducing TLR9-dependent type I IFN production in response to apoptotic DNA. In diseases involving TLR9 hyper-activities, such as psoriasis and arthritis [42, 87], TLR9 may be hyperactivated due to altered DNase II digestion of the released self-DNA. DNA binding proteins such as LL37 and HMGBs may contribute to such alteration by facilitating DNA cleavage by DNase II. Therapeutic intervention targeting these DNA binding proteins may thus avoid TLR9 hyperactivation and relieve disease severity. In cell types that express a large amount of TLR9, for instance, the pDCs, it is interesting to examine any modulation of DNase II-dependent DNA digestion when TLR9-triggered diseases develop.

In diseases caused by DNA viruses, TLR9 plays a protective role in confining the infection, and this is achieved by the induction of type I IFN [97]. Viruses such as herpes simplex viruses (HSVs) [17, 98, 99] and murine cytomegalovirus (MCMV) [100] stimulate IFN-α release from pDCs in a TLR9-dependent manner at the early phase of infection. The type I IFN released is important in subsequent induction of anti-HSV cytotoxic T cells [101]. Therefore, from the results obtained in this study,

DNase II is likely to be indispensable in promoting TLR9-dependent IFN production in mice infected with these viruses. The importance of DNase II in anti-viral responses may be studied by infecting the control or DNase II conditional knockout mice with HSVs or MCMV, and their survival examined.

Although CpG ODNs are synthetic ligands, they are widely used as an effective vaccine adjuvant against tumors or infectious diseases, due to their ability to induce prominent TLR9-dependent innate and adaptive immune responses [21, 22, 102, 103]. All the three classes of CpG ODNs, CpG-A, CpG-B and CpG-C, have been shown to induce cytotoxic or memory T cell responses when used as the adjuvant [21, 104]. CpG-A induces a large amount of type I IFN by virtue of forming tertiary structures [32, 105], and is shown to be superior to CpG-B in enhancing memory CD8+ T cell response and cytotoxicity [36, 103]. Besides, administration of CpG-A, but not CpG-B, improved the clinical outcome in healthy and immunocompromised primates against *Leishmania major* challenge [106]. Similar conclusion is also found in human immunodeficiency virus (HIV)-infected individuals, in which CpG-A activates pDCs to produce IFN-α in the patients [107] and this is important in suppressing HIV replication [108]. CpG-A is suggested to be a significantly better immune adjuvant *in vivo* compared with CpG-B [109]. However, due to the difficulty in maintaining a uniform higher-order multimeric CpG-A structure clinically without aggregation or precipitation, an effective thermolytic prodrug form of CpG-A has been developed [110]. A recent study shows that encapsulating such CpG-A prodrug in a special synthetic nanoparticle core enable the induction of antigen-specific T cell responses [111]. The nanoparticle core protects the adjuvant/vaccine until they are delivered to the large intestine. This strategy induces a protective immune response in subsequent viral challenges [111]. Besides, since CpG-A is potent in inducing type I

IFN in dendritic cells, which in turn activates NK cells [28, 31], administrating CpG-A alone in a murine model of human melanoma induces long-term survival of the mice [31]. Concerning the ability of CpG-A to induce Th1 responses, CpG DNA is suggested to be useful in treating asthma and allergic diseases [112]. In addition, a melanoma-specific antigen mixed with CpG-A-coated nanoparticles has been found to induce strong T cell responses in a clinical trial [113]. To mimic the IFN-α inducing property of CpG-A, coating CpG-B sequence on synthetic nanoparticles is also shown to induce CpG-A-like responses in cells, which also acts as a potent vaccine adjuvant in mouse models [114, 115]. In light of the essential role of DNase II in facilitating TLR9 responses to CpG-A in cDC and pDC, DNase II may be important in mediating the anti-viral or anti-tumor effect of various vaccines as mentioned above. It may be intriguing to study the cytotoxic T cell responses in vaccinated DNase II-deficient mice after infection *in vivo*.

In retrospect, the reason for the identification of CpG-A as a potent IFN-inducing ODN [29] may be the result of the selection for interacting with DNase II, as well as it can be efficiently transported to the endosome or lysosome to activate TLR9.

The present study revealed a novel role of DNase II in TLR9-dependent CpG-A responses, my findings may contribute to understanding the mechanism of actions in some drugs or vaccines that involve the use of CpG-A.

5. Reference

1 Medzhitov, R. and Janeway, C. A. (1997) Innate immunity: the virtues of a nonclonal system of recognition. Cell. **91**, 295-298

2 Medzhitov, R. and Janeway, C. (2000) Innate immunity. N Engl J Med. **343**, 338-344

3 Cooper, M. D. and Alder, M. N. (2006) The evolution of adaptive immune systems. Cell. **124**, 815-822

4 Batista, F. D. and Harwood, N. E. (2009) The who, how and where of antigen presentation to B cells. Nat Rev Immunol. **9**, 15-27

5 Guermonprez, P., Valladeau, J., Zitvogel, L., Théry, C. and Amigorena, S. (2002) Antigen presentation and T cell stimulation by dendritic cells. Annu Rev Immunol. **20**, 621-667

6 Bernasconi, N. L., Traggiai, E. and Lanzavecchia, A. (2002) Maintenance of serological memory by polyclonal activation of human memory B cells. Science. **298**, 2199-2202

7 MacLeod, H. and Wetzler, L. M. (2007) T cell activation by TLRs: a role for TLRs in the adaptive immune response. Sci STKE. **2007**, pe48

8 Keating, S. E., Baran, M. and Bowie, A. G. (2011) Cytosolic DNA sensors regulating type I interferon induction. Trends Immunol. **32**, 574-581

9 Sun, L., Wu, J., Du, F., Chen, X. and Chen, Z. J. (2013) Cyclic GMP-AMP synthase is a cytosolic DNA sensor that activates the type I interferon pathway. Science. **339**, 786-791

10 Wu, J., Sun, L., Chen, X., Du, F., Shi, H., Chen, C. and Chen, Z. J. (2013) Cyclic GMP-AMP is an endogenous second messenger in innate immune signaling by cytosolic DNA. Science. **339**, 826-830

11 Panne, D. (2013) Immunology: Cytosolic DNA sensing unraveled. Nat Chem Biol. **9**, 533-534

12 Hashimoto, C., Hudson, K. L. and Anderson, K. V. (1988) The Toll gene of Drosophila, required for dorsal-ventral embryonic polarity, appears to encode a transmembrane protein. Cell. **52**, 269-279

13 Medzhitov, R., Preston-Hurlburt, P. and Janeway, C. A. (1997) A human homologue of the Drosophila Toll protein signals activation of adaptive immunity. Nature. **388**, 394-397

14 Akira, S. and Takeda, K. (2004) Toll-like receptor signalling. Nat Rev Immunol. **4**, 499-511

15 Montero Vega, M. T. and de Andrés Martín, A. (2008) Toll-like receptors: a family of innate sensors of danger that alert and drive immunity. Allergol Immunopathol (Madr). **36**, 347-357

16 Hemmi, H., Takeuchi, O., Kawai, T., Kaisho, T., Sato, S., Sanjo, H., Matsumoto, M., Hoshino, K., Wagner, H., Takeda, K. and Akira, S. (2000) A Toll-like receptor recognizes bacterial DNA. Nature. **408**, 740-745

17 Lund, J., Sato, A., Akira, S., Medzhitov, R. and Iwasaki, A. (2003) Toll-like receptor 9-mediated recognition of Herpes simplex virus-2 by plasmacytoid dendritic cells. J Exp Med. **198**, 513-520

18 Chu, R. S., Targoni, O. S., Krieg, A. M., Lehmann, P. V. and Harding, C. V. (1997) CpG oligodeoxynucleotides act as adjuvants that switch on T helper 1 (Th1) immunity. J Exp Med. **186**, 1623-1631

19 Sun, S., Zhang, X., Tough, D. F. and Sprent, J. (1998) Type I interferon-mediated stimulation of T cells by CpG DNA. J Exp Med. **188**, 2335-2342

20 Roman, M., Martin-Orozco, E., Goodman, J. S., Nguyen, M. D., Sato, Y., Ronaghy, A., Kornbluth, R. S., Richman, D. D., Carson, D. A. and Raz, E. (1997) Immunostimulatory DNA sequences function as T helper-1-promoting adjuvants. Nat Med. **3**, 849-854

21 Bode, C., Zhao, G., Steinhagen, F., Kinjo, T. and Klinman, D. M. (2011) CpG DNA as a vaccine adjuvant. Expert Rev Vaccines. **10**, 499-511

22 Ballas, Z. K., Krieg, A. M., Warren, T., Rasmussen, W., Davis, H. L., Waldschmidt, M. and Weiner, G. J. (2001) Divergent therapeutic and immunologic effects of oligodeoxynucleotides with distinct CpG motifs. J Immunol. **167**, 4878-4886

23 Sato, Y., Roman, M., Tighe, H., Lee, D., Corr, M., Nguyen, M. D., Silverman, G. J., Lotz, M., Carson, D. A. and Raz, E. (1996) Immunostimulatory DNA sequences necessary for effective intradermal gene immunization. Science. **273**, 352-354

24 Krieg, A. M., Yi, A. K., Schorr, J. and Davis, H. L. (1998) The role of CpG dinucleotides in DNA vaccines. Trends Microbiol. **6**, 23-27

25 Krieg, A. M., Yi, A. K., Matson, S., Waldschmidt, T. J., Bishop, G. A., Teasdale, R., Koretzky, G. A. and Klinman, D. M. (1995) CpG motifs in bacterial DNA trigger direct B-cell activation. Nature. **374**, 546-549

26 Guzylack-Piriou, L., Balmelli, C., McCullough, K. C. and Summerfield, A. (2004) Type-A CpG oligonucleotides activate exclusively porcine natural interferon-producing cells to secrete interferon-alpha, tumour necrosis factor-alpha and interleukin-12. Immunology. **112**, 28-37

27 Krieg, A. M. (2002) CpG motifs in bacterial DNA and their immune effects. Annu Rev Immunol. **20**, 709-760

28 Vollmer, J., Weeratna, R., Payette, P., Jurk, M., Schetter, C., Laucht, M., Wader, T., Tluk, S., Liu, M., Davis, H. L. and Krieg, A. M. (2004) Characterization of three CpG oligodeoxynucleotide classes with distinct immunostimulatory activities. Eur J Immunol. **34**, 251-262

29 Krug, A., Rothenfusser, S., Hornung, V., Jahrsdörfer, B., Blackwell, S., Ballas, Z. K., Endres, S., Krieg, A. M. and Hartmann, G. (2001) Identification of CpG oligonucleotide sequences with high induction of IFN-alpha/beta in plasmacytoid dendritic cells. Eur J Immunol. **31**, 2154-2163

30 Verthelyi, D., Ishii, K. J., Gursel, M., Takeshita, F. and Klinman, D. M. (2001) Human peripheral blood cells differentially recognize and respond to two distinct CPG motifs. J Immunol. **166**, 2372-2377

31 Ballas, Z. K. (2007) Modulation of NK cell activity by CpG oligodeoxynucleotides. Immunol Res. **39**, 15-21

32 Kerkmann, M., Costa, L. T., Richter, C., Rothenfusser, S., Battiany, J., Hornung, V., Johnson, J., Englert, S., Ketterer, T., Heckl, W., Thalhammer, S., Endres, S. and Hartmann, G. (2005) Spontaneous formation of nucleic acid-based nanoparticles is responsible for high interferon-alpha induction by CpG-A in plasmacytoid dendritic cells. J Biol Chem. **280**, 8086-8093

33 Wang, D., Zhang, S., Li, L., Liu, X., Mei, K. and Wang, X. (2010) Structural insights into the assembly and activation of IL-1β with its receptors. Nat Immunol. **11**, 905-911

34 Valanne, S., Wang, J. H. and Rämet, M. (2011) The Drosophila Toll signaling pathway. J Immunol. **186**, 649-656

35 Akira, S., Uematsu, S. and Takeuchi, O. (2006) Pathogen recognition and innate immunity. Cell. **124**, 783-801

36 Krug, A., Rothenfusser, S., Selinger, S., Bock, C., Kerkmann, M., Battiany, J., Sarris, A., Giese, T., Speiser, D., Endres, S. and Hartmann, G. (2003) CpG-A oligonucleotides induce a monocyte-derived dendritic cell-like phenotype that preferentially activates CD8 T cells. J Immunol. **170**, 3468-3477

37 Roda, J. M., Parihar, R. and Carson, W. E. (2005) CpG-containing oligodeoxynucleotides act through TLR9 to enhance the NK cell cytokine response to antibody-coated tumor cells. J Immunol. **175**, 1619-1627

38 Zhang, X., He, P., Hu, Z., Wang, X. and Liang, Z. (2011) Enhanced specific immune responses by CpG DNA in mice immunized with recombinant hepatitis B surface antigen and HB vaccine. Virol J. **8**, 78

39 Duggan, J. M., You, D., Cleaver, J. O., Larson, D. T., Garza, R. J., Guzmán Pruneda, F. A., Tuvim, M. J., Zhang, J., Dickey, B. F. and Evans, S. E. (2011) Synergistic interactions of TLR2/6 and TLR9 induce a high level of resistance to lung infection in mice. J Immunol. **186**, 5916-5926

40 Brinkmann, M. M., Spooner, E., Hoebe, K., Beutler, B., Ploegh, H. L. and Kim, Y. M. (2007) The interaction between the ER membrane protein UNC93B and TLR3, 7, and 9 is crucial for TLR signaling. J Cell Biol. **177**, 265-275

41 Matsumoto, F., Saitoh, S., Fukui, R., Kobayashi, T., Tanimura, N., Konno, K., Kusumoto, Y., Akashi-Takamura, S. and Miyake, K. (2008) Cathepsins are required for Toll-like receptor 9 responses. Biochem Biophys Res Commun. **367**, 693-699

42 Asagiri, M., Hirai, T., Kunigami, T., Kamano, S., Gober, H. J., Okamoto, K., Nishikawa, K., Latz, E., Golenbock, D. T., Aoki, K., Ohya, K., Imai, Y., Morishita, Y., Miyazono, K., Kato, S., Saftig, P. and Takayanagi, H. (2008) Cathepsin K-dependent toll-like receptor 9 signaling revealed in experimental arthritis. Science. **319**, 624-627

43 Ewald, S. E., Lee, B. L., Lau, L., Wickliffe, K. E., Shi, G. P., Chapman, H. A. and Barton, G. M. (2008) The ectodomain of Toll-like receptor 9 is cleaved to generate a functional receptor. Nature. **456**, 658-662

44 Park, B., Brinkmann, M. M., Spooner, E., Lee, C. C., Kim, Y. M. and Ploegh, H. L. (2008) Proteolytic cleavage in an endolysosomal compartment is required for activation of Toll-like receptor 9. Nat Immunol. **9**, 1407-1414

45 Kawai, T. and Akira, S. (2010) The role of pattern-recognition receptors in innate immunity: update on Toll-like receptors. Nat Immunol. **11**, 373-384

46 Muroi, M. and Tanamoto, K. (2008) TRAF6 distinctively mediates MyD88- and IRAK-1-induced activation of NF-kappaB. J Leukoc Biol. **83**, 702-707

47 Deng, L., Wang, C., Spencer, E., Yang, L., Braun, A., You, J., Slaughter, C., Pickart, C. and Chen, Z. J. (2000) Activation of the IkappaB kinase complex by TRAF6 requires a dimeric ubiquitin-conjugating enzyme complex and a unique polyubiquitin chain. Cell. **103**, 351-361

48 Arthur, J. S. and Ley, S. C. (2013) Mitogen-activated protein kinases in innate immunity. Nat Rev Immunol. **13**, 679-692

49 Häcker, H. and Karin, M. (2006) Regulation and function of IKK and IKK-related kinases. Sci STKE. **2006**, re13

50 Negishi, H., Fujita, Y., Yanai, H., Sakaguchi, S., Ouyang, X., Shinohara, M., Takayanagi, H., Ohba, Y., Taniguchi, T. and Honda, K. (2006) Evidence for

licensing of IFN-gamma-induced IFN regulatory factor 1 transcription factor by MyD88 in Toll-like receptor-dependent gene induction program. Proc Natl Acad Sci U S A. **103**, 15136-15141

51 Schmitz, F., Heit, A., Guggemoos, S., Krug, A., Mages, J., Schiemann, M., Adler, H., Drexler, I., Haas, T., Lang, R. and Wagner, H. (2007) Interferon-regulatory-factor 1 controls Toll-like receptor 9-mediated IFN-beta production in myeloid dendritic cells. Eur J Immunol. **37**, 315-327

52 Honda, K., Ohba, Y., Yanai, H., Negishi, H., Mizutani, T., Takaoka, A., Taya, C. and Taniguchi, T. (2005) Spatiotemporal regulation of MyD88-IRF-7 signalling for robust type-I interferon induction. Nature. **434**, 1035-1040

53 Yasutomo, K., Horiuchi, T., Kagami, S., Tsukamoto, H., Hashimura, C., Urushihara, M. and Kuroda, Y. (2001) Mutation of DNASE1 in people with systemic lupus erythematosus. Nat Genet. **28**, 313-314

54 Shin, H. D., Park, B. L., Kim, L. H., Lee, H. S., Kim, T. Y. and Bae, S. C. (2004) Common DNase I polymorphism associated with autoantibody production among systemic lupus erythematosus patients. Hum Mol Genet. **13**, 2343-2350

55 Napirei, M., Karsunky, H., Zevnik, B., Stephan, H., Mannherz, H. G. and Möröy, T. (2000) Features of systemic lupus erythematosus in Dnase1-deficient mice. Nat Genet. **25**, 177-181

56 Ahn, J., Gutman, D., Saijo, S. and Barber, G. N. (2012) STING manifests self DNA-dependent inflammatory disease. Proc Natl Acad Sci U S A. **109**, 19386-19391

57 Kawane, K., Fukuyama, H., Kondoh, G., Takeda, J., Ohsawa, Y., Uchiyama, Y. and Nagata, S. (2001) Requirement of DNase II for definitive erythropoiesis in the mouse fetal liver. Science. **292**, 1546-1549

58 Yoshida, H., Okabe, Y., Kawane, K., Fukuyama, H. and Nagata, S. (2005) Lethal anemia caused by interferon-beta produced in mouse embryos carrying undigested DNA. Nat Immunol. **6**, 49-56

59 Kawane, K., Ohtani, M., Miwa, K., Kizawa, T., Kanbara, Y., Yoshioka, Y., Yoshikawa, H. and Nagata, S. (2006) Chronic polyarthritis caused by mammalian DNA that escapes from degradation in macrophages. Nature. **443**, 998-1002

60 Shin, H. D., Park, B. L., Cheong, H. S., Lee, H. S., Jun, J. B. and Bae, S. C. (2005) DNase II polymorphisms associated with risk of renal disorder among systemic lupus erythematosus patients. J Hum Genet. **50**, 107-111

61 White, S. and Rosen, A. (2003) Apoptosis in systemic lupus erythematosus. Curr Opin Rheumatol. **15**, 557-562

62 Kawane, K., Fukuyama, H., Yoshida, H., Nagase, H., Ohsawa, Y., Uchiyama, Y., Okada, K., Iida, T. and Nagata, S. (2003) Impaired thymic development in mouse embryos deficient in apoptotic DNA degradation. Nat Immunol. **4**, 138-144

63 Gall, A., Treuting, P., Elkon, K. B., Loo, Y. M., Gale, M., Barber, G. N. and Stetson, D. B. (2012) Autoimmunity initiates in nonhematopoietic cells and progresses via lymphocytes in an interferon-dependent autoimmune disease. Immunity. **36**, 120-131

64 Barizzone, N., Monti, S., Mellone, S., Godi, M., Marchini, M., Scorza, R., Danieli, M. G. and D'Alfonso, S. (2013) Rare variants in the TREX1 gene and susceptibility to autoimmune diseases. Biomed Res Int. **2013**, 471703

65 Blasius, A. L. and Beutler, B. (2010) Intracellular toll-like receptors. Immunity. **32**, 305-315

66 Oka, T., Hikoso, S., Yamaguchi, O., Taneike, M., Takeda, T., Tamai, T., Oyabu, J., Murakawa, T., Nakayama, H., Nishida, K., Akira, S., Yamamoto, A., Komuro, I. and Otsu, K. (2012) Mitochondrial DNA that escapes from autophagy causes inflammation and heart failure. Nature. **485**, 251-255

67 Okabe, Y., Kawane, K., Akira, S., Taniguchi, T. and Nagata, S. (2005) Toll-like receptor-independent gene induction program activated by mammalian DNA escaped from apoptotic DNA degradation. J Exp Med. **202**, 1333-1339

68 Evans, C. J. and Aguilera, R. J. (2003) DNase II: genes, enzymes and function. Gene. **322**, 1-15

69 Sasai, M., Linehan, M. M. and Iwasaki, A. (2010) Bifurcation of Toll-like receptor 9 signaling by adaptor protein 3. Science. **329**, 1530-1534

70 Chockalingam, A., Rose, W. A., Hasan, M., Ju, C. H. and Leifer, C. A. (2012) Cutting edge: a TLR9 cytoplasmic tyrosine motif is selectively required for proinflammatory cytokine production. J Immunol. **188**, 527-530

71 Onji, M., Kanno, A., Saitoh, S., Fukui, R., Motoi, Y., Shibata, T., Matsumoto, F., Lamichhane, A., Sato, S., Kiyono, H., Yamamoto, K. and Miyake, K. (2013) An essential role for the N-terminal fragment of Toll-like receptor 9 in DNA sensing. Nat Commun. **4**, 1949

72 Van Amersfoort, E. S. and Van Strijp, J. A. (1994) Evaluation of a flow cytometric fluorescence quenching assay of phagocytosis of sensitized sheep erythrocytes by polymorphonuclear leukocytes. Cytometry. **17**, 294-301

73 Honda, K., Yanai, H., Takaoka, A. and Taniguchi, T. (2005) Regulation of the type I IFN induction: a current view. Int Immunol. **17**, 1367-1378

74 Cheng, Y. C., Hsueh, C. C., Lu, S. C. and Liao, T. H. (2006) Identification of three crucial histidine residues (His115, His132 and His297) in porcine deoxyribonuclease II. Biochem J. **398**, 177-185

75 Counis, M. F. and Torriglia, A. (2006) Acid DNases and their interest among apoptotic endonucleases. Biochimie. **88**, 1851-1858

76 Fearon, K., Marshall, J. D., Abbate, C., Subramanian, S., Yee, P., Gregorio, J., Teshima, G., Ott, G., Tuck, S., Van Nest, G. and Coffman, R. L. (2003) A minimal human immunostimulatory CpG motif that potently induces IFN-gamma and IFN-alpha production. Eur J Immunol. **33**, 2114-2122

77 Hartmann, G., Battiany, J., Poeck, H., Wagner, M., Kerkmann, M., Lubenow, N., Rothenfusser, S. and Endres, S. (2003) Rational design of new CpG oligonucleotides that combine B cell activation with high IFN-alpha induction in plasmacytoid dendritic cells. Eur J Immunol. **33**, 1633-1641

78 Ohkouchi, S., Shibata, M., Sasaki, M., Koike, M., Safig, P., Peters, C., Nagata, S. and Uchiyama, Y. (2013) Biogenesis and proteolytic processing of lysosomal DNase II. PLoS One. **8**, e59148

79 Guasch, R. M., Guerri, C. and O'Connor, J. E. (1995) Study of surface carbohydrates on isolated Golgi subfractions by fluorescent-lectin binding and flow cytometry. Cytometry. **19**, 112-118

80 Iida, H. and Page, E. (1989) Localization of wheat-germ agglutinin-binding sites in the Golgi complex of cultured rat atrial myocytes. Cell Tissue Res. **257**, 325-331

81 Kanazawa, T., Takematsu, H., Yamamoto, A., Yamamoto, H. and Kozutsumi, Y. (2008) Wheat germ agglutinin stains dispersed post-golgi vesicles after treatment with the cytokinesis inhibitor psychosine. J Cell Physiol. **215**, 517-525

82 Guiducci, C., Ott, G., Chan, J. H., Damon, E., Calacsan, C., Matray, T., Lee, K. D., Coffman, R. L. and Barrat, F. J. (2006) Properties regulating the nature of the plasmacytoid dendritic cell response to Toll-like receptor 9 activation. J Exp Med. **203**, 1999-2008

83 Ivanov, S., Dragoi, A. M., Wang, X., Dallacosta, C., Louten, J., Musco, G., Sitia, G., Yap, G. S., Wan, Y., Biron, C. A., Bianchi, M. E., Wang, H. and Chu, W. M. (2007) A novel role for HMGB1 in TLR9-mediated inflammatory responses to CpG-DNA. Blood. **110**, 1970-1981

84 Latz, E., Schoenemeyer, A., Visintin, A., Fitzgerald, K. A., Monks, B. G., Knetter, C. F., Lien, E., Nilsen, N. J., Espevik, T. and Golenbock, D. T. (2004) TLR9 signals after translocating from the ER to CpG DNA in the lysosome. Nat Immunol. **5**, 190-198

85 Haas, T., Schmitz, F., Heit, A. and Wagner, H. (2009) Sequence independent interferon-alpha induction by multimerized phosphodiester DNA depends on spatial regulation of Toll-like receptor-9 activation in plasmacytoid dendritic cells. Immunology. **126**, 290-298

86 Koltover, I., Salditt, T., Rädler, J. O. and Safinya, C. R. (1998) An inverted hexagonal phase of cationic liposome-DNA complexes related to DNA release and delivery. Science. **281**, 78-81

87 Lande, R., Gregorio, J., Facchinetti, V., Chatterjee, B., Wang, Y. H., Homey, B., Cao, W., Su, B., Nestle, F. O., Zal, T., Mellman, I., Schröder, J. M., Liu, Y. J. and Gilliet, M. (2007) Plasmacytoid dendritic cells sense self-DNA coupled with antimicrobial peptide. Nature. **449**, 564-569

88 Nestle, F. O., Conrad, C., Tun-Kyi, A., Homey, B., Gombert, M., Boyman, O., Burg, G., Liu, Y. J. and Gilliet, M. (2005) Plasmacytoid predendritic cells initiate psoriasis through interferon-alpha production. J Exp Med. **202**, 135-143

89 Gilliet, M., Cao, W. and Liu, Y. J. (2008) Plasmacytoid dendritic cells: sensing nucleic acids in viral infection and autoimmune diseases. Nat Rev Immunol. **8**, 594-606

90 Tian, J., Avalos, A. M., Mao, S. Y., Chen, B., Senthil, K., Wu, H., Parroche, P., Drabic, S., Golenbock, D., Sirois, C., Hua, J., An, L. L., Audoly, L., La Rosa, G., Bierhaus, A., Naworth, P., Marshak-Rothstein, A., Crow, M. K., Fitzgerald, K. A., Latz, E., Kiener, P. A. and Coyle, A. J. (2007) Toll-like receptor 9-dependent activation by DNA-containing immune complexes is mediated by HMGB1 and RAGE. Nat Immunol. **8**, 487-496

91 Yanai, H., Ban, T., Wang, Z., Choi, M. K., Kawamura, T., Negishi, H., Nakasato, M., Lu, Y., Hangai, S., Koshiba, R., Savitsky, D., Ronfani, L., Akira, S., Bianchi, M. E., Honda, K., Tamura, T., Kodama, T. and Taniguchi, T. (2009) HMGB proteins function as universal sentinels for nucleic-acid-mediated innate immune responses. Nature. **462**, 99-103

92 Bonifacino, J. S. and Rojas, R. (2006) Retrograde transport from endosomes to the trans-Golgi network. Nat Rev Mol Cell Biol. **7**, 568-579

93 Henne, W. M., Buchkovich, N. J. and Emr, S. D. (2011) The ESCRT pathway. Dev Cell. **21**, 77-91

94 Kawane, K., Tanaka, H., Kitahara, Y., Shimaoka, S. and Nagata, S. (2010) Cytokine-dependent but acquired immunity-independent arthritis caused by DNA escaped from degradation. Proc Natl Acad Sci U S A. **107**, 19432-19437

95 Abe, T., Harashima, A., Xia, T., Konno, H., Konno, K., Morales, A., Ahn, J., Gutman, D. and Barber, G. N. (2013) STING recognition of cytoplasmic DNA instigates cellular defense. Mol Cell. **50**, 5-15

96 Cai, X., Chiu, Y. H. and Chen, Z. J. (2014) The cGAS-cGAMP-STING Pathway of Cytosolic DNA Sensing and Signaling. Mol Cell. **54**, 289-296

97 Perry, A. K., Chen, G., Zheng, D., Tang, H. and Cheng, G. (2005) The host type I interferon response to viral and bacterial infections. Cell Res. **15**, 407-422

98 Krug, A., Luker, G. D., Barchet, W., Leib, D. A., Akira, S. and Colonna, M. (2004) Herpes simplex virus type 1 activates murine natural interferon-producing cells through toll-like receptor 9. Blood. **103**, 1433-1437

99 Rasmussen, S. B., Sørensen, L. N., Malmgaard, L., Ank, N., Baines, J. D., Chen, Z. J. and Paludan, S. R. (2007) Type I interferon production during herpes simplex virus infection is controlled by cell-type-specific viral recognition through Toll-like receptor 9, the mitochondrial antiviral signaling protein pathway, and novel recognition systems. J Virol. **81**, 13315-13324

100 Delale, T., Paquin, A., Asselin-Paturel, C., Dalod, M., Brizard, G., Bates, E. E., Kastner, P., Chan, S., Akira, S., Vicari, A., Biron, C. A., Trinchieri, G. and

Brière, F. (2005) MyD88-dependent and -independent murine cytomegalovirus sensing for IFN-alpha release and initiation of immune responses in vivo. J Immunol. **175**, 6723-6732

101 Yoneyama, H., Matsuno, K., Toda, E., Nishiwaki, T., Matsuo, N., Nakano, A., Narumi, S., Lu, B., Gerard, C., Ishikawa, S. and Matsushima, K. (2005) Plasmacytoid DCs help lymph node DCs to induce anti-HSV CTLs. J Exp Med. **202**, 425-435

102 Cui, J., Shin, T., Kawano, T., Sato, H., Kondo, E., Toura, I., Kaneko, Y., Koseki, H., Kanno, M. and Taniguchi, M. (1997) Requirement for Valpha14 NKT cells in IL-12-mediated rejection of tumors. Science. **278**, 1623-1626

103 Rothenfusser, S., Hornung, V., Ayyoub, M., Britsch, S., Towarowski, A., Krug, A., Sarris, A., Lubenow, N., Speiser, D., Endres, S. and Hartmann, G. (2004) CpG-A and CpG-B oligonucleotides differentially enhance human peptide-specific primary and memory CD8+ T-cell responses in vitro. Blood. **103**, 2162-2169

104 Wille-Reece, U., Flynn, B. J., Loré, K., Koup, R. A., Miles, A. P., Saul, A., Kedl, R. M., Mattapallil, J. J., Weiss, W. R., Roederer, M. and Seder, R. A. (2006) Toll-like receptor agonists influence the magnitude and quality of memory T cell responses after prime-boost immunization in nonhuman primates. J Exp Med. **203**, 1249-1258

105 Wu, C. C., Lee, J., Raz, E., Corr, M. and Carson, D. A. (2004) Necessity of oligonucleotide aggregation for toll-like receptor 9 activation. J Biol Chem. **279**, 33071-33078

106 Verthelyi, D., Gursel, M., Kenney, R. T., Lifson, J. D., Liu, S., Mican, J. and Klinman, D. M. (2003) CpG oligodeoxynucleotides protect normal and SIV-infected macaques from Leishmania infection. J Immunol. **170**, 4717-4723

107 Martinson, J. A., Tenorio, A. R., Montoya, C. J., Al-Harthi, L., Gichinga, C. N., Krieg, A. M., Baum, L. L. and Landay, A. L. (2007) Impact of class A, B and C CpG-oligodeoxynucleotides on in vitro activation of innate immune cells in human immunodeficiency virus-1 infected individuals. Immunology. **120**, 526-535

108 Schmidt, B., Ashlock, B. M., Foster, H., Fujimura, S. H. and Levy, J. A. (2005) HIV-infected cells are major inducers of plasmacytoid dendritic cell interferon production, maturation, and migration. Virology. **343**, 256-266

109 Gürsel, M., Verthelyi, D., Gürsel, I., Ishii, K. J. and Klinman, D. M. (2002) Differential and competitive activation of human immune cells by distinct classes of CpG oligodeoxynucleotide. J Leukoc Biol. **71**, 813-820

110 Puig, M., Grajkowski, A., Boczkowska, M., Ausín, C., Beaucage, S. L. and Verthelyi, D. (2006) Use of thermolytic protective groups to prevent G-tetrad formation in CpG ODN type D: structural studies and immunomodulatory activity in primates. Nucleic Acids Res. **34**, 6488-6495

111 Zhu, Q., Talton, J., Zhang, G., Cunningham, T., Wang, Z., Waters, R. C., Kirk, J., Eppler, B., Klinman, D. M., Sui, Y., Gagnon, S., Belyakov, I. M., Mumper, R. J. and Berzofsky, J. A. (2012) Large intestine-targeted, nanoparticle-releasing oral vaccine to control genitorectal viral infection. Nat Med. **18**, 1291-1296

112 Fonseca, D. E. and Kline, J. N. (2009) Use of CpG oligonucleotides in treatment of asthma and allergic disease. Adv Drug Deliv Rev. **61**, 256-262

113 Speiser, D. E., Schwarz, K., Baumgaertner, P., Manolova, V., Devevre, E., Sterry, W., Walden, P., Zippelius, A., Conzett, K. B., Senti, G., Voelter, V., Cerottini, J. P., Guggisberg, D., Willers, J., Geldhof, C., Romero, P., Kündig, T., Knuth, A., Dummer, R., Trefzer, U. and Bachmann, M. F. (2010) Memory and effector CD8 T-cell responses after nanoparticle vaccination of melanoma patients. J Immunother. **33**, 848-858

114 Gungor, B., Yagci, F. C., Tincer, G., Bayyurt, B., Alpdundar, E., Yildiz, S., Ozcan, M., Gursel, I. and Gursel, M. (2014) CpG ODN Nanorings Induce IFNα from Plasmacytoid Dendritic Cells and Demonstrate Potent Vaccine Adjuvant Activity. Sci Transl Med. **6**, 235ra261

115 de Titta, A., Ballester, M., Julier, Z., Nembrini, C., Jeanbart, L., van der Vlies, A. J., Swartz, M. A. and Hubbell, J. A. (2013) Nanoparticle conjugation of CpG enhances adjuvancy for cellular immunity and memory recall at low dose. Proc Natl Acad Sci U S A. **110**, 19902-19907